11-4-2019

Spatiotemporal Analysis Of Lake Water Quality Indicators On Small Lakes, Lake Bloomington And Evergreen Lake In Central Illinois, Using Satellite Remote Sensing

Gare Ambrose-Igho
Illinois State University, gareigho@yahoo.co.uk

SPATIOTEMPORAL ANALYSIS OF LAKE WATER QUALITY INDICATORS ON SMALL LAKES, LAKE BLOOMINGTON AND EVERGREEN LAKE IN CENTRAL ILLINOIS, USING SATELLITE REMOTE SENSING

GARE AMBROSE-IGHO

53 Pages

This research explores the use of Sentinel-2 satellite to determine the spatiotemporal patterns of lake water quality indicators (e.g. chlorophyll *a*) in Lake Bloomington and Evergreen Lake. Lake water quality issues related to algal blooms is a serious problem in basins with abundant agricultural lands causing harmful effects to freshwater ecosystems such as pollution of beaches, taste and odor problems in drinking water, depletion of oxygen levels causing fish kills and the issue of water exceeding safe drinking water standards. Developing monitoring techniques using various water quality indicators of algal blooms is crucial. In this project, remote sensing and field sampling methods were employed to assess the state of water quality of two small lakes, Lake Bloomington and Evergreen Lake, in Central Illinois. Water samples were collected from selected locations from the lakes to test for various water quality variables including nitrate, phosphorus and chlorophyll *a.* An exo sonde instrument and secchi disk was used to measure additional water quality parameters such as turbidity, secchi depth, and temperature. Concurrent satellite images obtained from Sentinel-2 with flyover with ±5 days were processed and analyzed, and the results were compared with field sampling data. Single and multiple pixel analyses were conducted on various algorithms such as Bottom-of-Atmosphere (BOA), Maximum Chlorophyll Index (MCI), and band ratios. These algorithms were tested to identify the best algorithm for estimating water quality parameters using satellite data for the two lakes. A regression analysis

was conducted to derive a linear model which was used to create water quality indicator maps that showed the spatial pattern of algae in the lakes. From the results of the research, Lake Bloomington was more turbid and had higher concentrations of chlorophyll *a* than Evergreen Lake. Except for band ratio of B1/B2 of Sentinel-2 data, a poor regression relationship between satellite and field water quality values was observed for Lake Bloomington. This poor relationship could be due to the high turbidity of the lake. Evergreen Lake, on the other hand, showed a stronger relationship between satellite values and chlorophyll *a*. Generally, spatial analysis reveals that chlorophyll *a* distribution was heterogeneous, and it increased from downstream areas to upstream areas.

KEYWORDS: algal bloom, chlorophyll *a*, remote sensing, Sentinel-2, turbidity, lake

SPATIOTEMPORAL ANALYSIS OF LAKE WATER QUALITY INDICATORS ON SMALL LAKES, LAKE BLOOMINGTON AND EVERGREEN LAKE IN CENTRAL ILLINOIS, USING SATELLITE REMOTE SENSING

GARE AMBROSE-IGHO

A Thesis Submitted in Partial
Fulfillment of the Requirements
for the Degree of

MASTER OF SCIENCE

Department of Geography, Geology, and the Environment

ILLINOIS STATE UNIVERSITY

2020

SPATIOTEMPORAL ANALYSIS OF LAKE WATER QUALITY INDICATORS ON SMALL LAKES, LAKE BLOOMINGTON AND EVERGREEN LAKE IN CENTRAL ILLINOIS, USING SATELLITE REMOTE SENSING

GARE AMBROSE-IGHO

COMMITTEE MEMBERS:

Wondwosen Seyoum, Co-chair

William L. Perry, Co-chair

Catherine O'Reilly

ACKNOWLEDGMENTS

I wish to acknowledge my committee members Wondwosen Seyoum, William L. Perry and Catherine O'Reilly, for their support and guidance during the thesis process. I would like to acknowledge Rick Twait with the City of Bloomington for the opportunity given to me to conduct this research on the lakes. I would also like to thank Illinois State Management Association (ILMA), the Graduate School and the Geological Society of America (GSA) for providing funds for this project.

Next, I must specially thank William L. Perry for his assistance with transporting the boat to the location of the two lakes and assisting in driving the boat as well as helping to collect water samples. I thank my colleagues; Prince Oware, Luis Martinez, Holly Gregorich and Linnea Johnson for their assistance with the field work.

I also greatly appreciate Illinois State University for the tuition waiver benefit while working at the University. Finally, I would like to make a special thank you to my family for understanding the commitment of pursuing my degree.

G.A.I

CONTENTS

TABLES

FIGURES

CHAPTER I: INTRODUCTION

Freshwater is the most important source of drinking water for the United States population and when there is a high concentration of algal blooms in the water, it degrades the quality of water by rendering it unfit for consumption or even recreational purposes (Hilborn et al., 2014). Algal blooms occur in freshwater when there is a sudden rise in the population of algae in the water body and it leads to changes in water (Glibert et al., 2005). Temperature, nitrogen and phosphorus have been identified as factors that may contribute to the occurrence of algal blooms in freshwater (Anderson et al., 2002; Carmichael, 2008; Havens, 2008). There are both harmless and harmful algal blooms (Glibert et al., 2005) and the most common harmful algal bloom (HAB) found in freshwater is the blue-green algae, also known as cyanobacteria (Hudnell, 2008). Cyanobacteria, like plants and true algae, can photosynthesize by using sunlight energy captured by chlorophyll *a* which it possesses. Cyanobacteria also need nutrients like nitrogen and phosphorus found in the water to grow and because of this, cyanobacteria may be more abundant in lakes, rivers and reservoirs where these nutrients are high (Bartram and Chorus, 1999). Unlike most plants, cyanobacteria can capture and fix nitrogen from the atmosphere (Braig IV et al., 2011). The impacts/issues of HABs are increasing globally and appear to increase with global changes such as climate change and human activities (Braig IV et al., 2011; Fu et al., 2012).

When assessing the suitability and availability of a reservoir or water source for drinking purposes, water quality is usually considered as an important factor (Raman and Twait, 1994).. Algae have a wide range of beneficial and harmful consequences on freshwater ecosystem and water quality (Stevenson, 2014). They serve as important sources of food for the lake ecosystem and are therefore important to the food web of freshwater ecosystems (Guo et al., 2016). Cyanobacteria produce toxins known as cyanotoxins (Carmichael, 2008) that have negative

impacts on freshwater ecosystem, the environment and human health. Some of these negative impacts include change of freshwater color and taste, change of and development of odor in freshwater, fish die-offs, anoxia and health risks for humans such as skin irritation, vomiting and in some cases death (Carmichael, 2008; Clark et al., 2017). Assessment of the suitability and availability of a reservoir for various purposes, including drinking purposes, usually involves monitoring of the reservoir and the concentration of algal blooms is usually an important indicator of degraded water quality (Richardson, 1996) and the aquatic ecosystem health. Field sampling methods have been used to monitor algae in freshwater for years. Due to the limitations associated with monitoring of lakes using field sampling methods only, new methods such as satellite remote sensing have been developed and used in addition to field methods to monitor lakes (Ritchie et al., 2003).

Satellite remote sensing serves as an effective complement to field sampling methods (Li and Li, 2004). Satellites have certain advantages over in-situ/field sampling methods. Satellite remote sensing provides a cost-effective and less time-consuming way to acquire information from lakes (Olmanson et al., 2002). The information acquired from this remote sensing method is spatially unbiased and allows for the collection of data from very large areas (Li and Li, 2004). Monitoring of lakes using conventional field sampling methods is expensive, dependent on the size of the lake and also time consuming (Li and Li, 2004), thus they are only used on small areas of the lake. Even though satellite remote sensing cannot be used to capture cyanotoxins present in cyanobacteria in lakes (Stumpf et al., 2016), concentration of algae can be quantified via chlorophyll *a* concentration using remote sensing (Clark et al., 2017; Richardson, 1996). Satellite image processing results have been successfully used to show the temporal and spatial distribution of chlorophyll *a*, phytoplankton biovolume and cyanobacteria biovolume in various lakes

(Isenstein et al., 2014). Remote sensing data have also been used to estimate the spatial distribution of Water Quality Parameters (WQPs) such as chlorophyll *a*, total phosphorus, and total nitrogen in rivers (Lim and Choi, 2015).

Monitoring of lakes using satellite remote sensing data is useful in estimating and understanding water quality problems (Kloiber et al., 2002). Remote sensing involves using satellites to capture information about objects on earth without having direct contact with them. Satellite remote sensing involves the extraction and interpretation of information from images acquired from the satellite which uses electromagnetic radiation (reflected or emitted from the Earth's surface) in various electromagnetic spectrum (Campbell and Wynne, 2011; Richards and Richards, 1999). Each object on earth possesses a unique intensity of radiation which is emitted or reflected. Remote sensing satellites are able to capture information reflected from objects on earth using sensors that have different wavelength bands (Gupta, 2017). Numerous remote sensing satellites including Landsat, Sentinel, MODIS have been launched and they are used to capture information from objects on earth including from water bodies including lakes. Data acquired using satellite remote sensing can be used to estimate algal bloom concentrations (Brezonik et al., 2005) in lakes by determining the concentration of chlorophyll *a* in the lake. However, satellite remote sensing can only be used to determine the spatial extent of algal blooms potential, further information is required to determine whether an algal bloom is a harmful algal bloom by comparing to data obtained from field sampling done on the lake with satellite remote sensing data (Park and Ruddick, 2007).

A new series of next-generation satellite program, Sentinel program, that provides continuous data to ensure that there are no gaps in ongoing studies has been launched by the European Space Agency (ESA). The Sentinel program was developed by the ESA to replace older

ESA's Earth observation missions that have reached retirement or currently nearing the end of their operational life span (Martimort et al., 2007). The Sentinel program is made up of 6 Sentinel missions (Sentinel 1 – 6), with each mission made up of two satellites. Sentinel-2 mission is composed of two polar-orbiting satellites (S2A and S2B) that provide high-resolution optical imagery (Djamai and Fernandes, 2018). The Sentinel-2 satellites have a 5-day overpass time which means that it passes across the same location in 5 days intervals. Sentinel-2A and Sentinel-2B were launched on 23 June 2015 and 7 March 2017 respectively, with a mission focused on land monitoring including vegetation, soil and coastal areas (Main-Knorn et al., 2015). Sentinel-2 has been used for various studies including the estimation of colored dissolved organic matter (Chen et al., 2017), retrieval of suspended particulate matter concentrations (Liu et al., 2017), mapping of phytoplankton blooms in lakes (Bresciani et al., 2018), and mapping of lake water quality (Toming et al., 2016).

Objectives, Question, and Hypothesis

1. Understand conditions that influence and facilitate chlorophyll *a* variability:

   What factors influence the spatial distribution of chlorophyll a?

   Variation is influenced by nutrients and temperature.

2. Compare satellite to field chlorophyll *a*.

   How well does the satellite imagery capture chlorophyll *a?*

   Satellite imagery will be a good predictor of chlorophyll *a*.

3. Predict lake water quality indicator variability using remote sensing:

   What is the spatial pattern of chlorophyll *a in the lakes?*

   Chlorophyll *a* concentration will vary spatially and temporally rather than have a homogenous distribution.

CHAPTER II: STUDY AREA

The study lakes, Lake Bloomington and Evergreen Lake, are in McClean County, Central Illinois (Figure 1). Lake Bloomington (LB) and Evergreen Lake (EV) serve as water supply reservoirs for the City of Bloomington. Evergreen Lake is larger in size and depth than Lake Bloomington. Lake Bloomington (Figure 1) is located 24 km North of Bloomington, Illinois in Hudson, Illinois, United States. It is a man-made lake built in 1929 by constructing an earth dam across Money Creek, with an original purpose of supplying Bloomington with a reliable, primary source of drinking water (Stall et al., 1958) and it presently supplies water to over 80,000 people. It is owned, maintained and operated by the city's water department (Roberts, 1948). In addition, Lake Bloomington is also used for recreational purposes and serves as host to over 220 residential sites (Raman and Twait, 1994). The lake has a surface area of 2.6 km^2, a drainage area of approximately 158 km^2, a storage capacity of about 8.3 million m^3 (2.2 billion gallons) and a mean depth of 3.9 m (Raman and Twait, 1994; Roberts, 1948; Stall et al., 1958).

Evergreen lake (Figure 1) is also located 24 km North of Bloomington, Illinois in Hudson, United States. It was built in 1971, by impounding Six Mile Creek where it meets with Mackinaw River, to increase the water supply to the City of Bloomington and for recreational purposes (Raman and Twait, 1994). The lake is owned by the City of Bloomington and is managed by the McLean County Department of Parks and Recreation. The lake has a surface area of 3.6km^2, a storage capacity of about 18.5million m^3 (4.9 billion gallons) and a mean depth of 5.1m (Meyers, 2014; Raman and Twait, 1994).

Money Creek and Six Mile Creek watersheds are the two primary tributaries of Lake Bloomington and Evergreen Lake respectively and are also major tributaries to Mackinaw River (Kelly et al., 1998). The Money Creek Watershed has a surface area of 181.07 km^2 while the Six

Mile Creek is 109.95 km^2. Their land uses are dominantly agriculture (corn and soybean) and rural grassland, with row crops covering 90% of the watersheds. Four glacial advances dominate the geological history of Illinois and as such, glaciers were very important in the development and formation of the soil types and terrains of McClean County (Hanna, 2013). The soil is poorly drained, very fertile, drought resistant and mostly silty clay loams and silt loams (Collman et al., 2002).

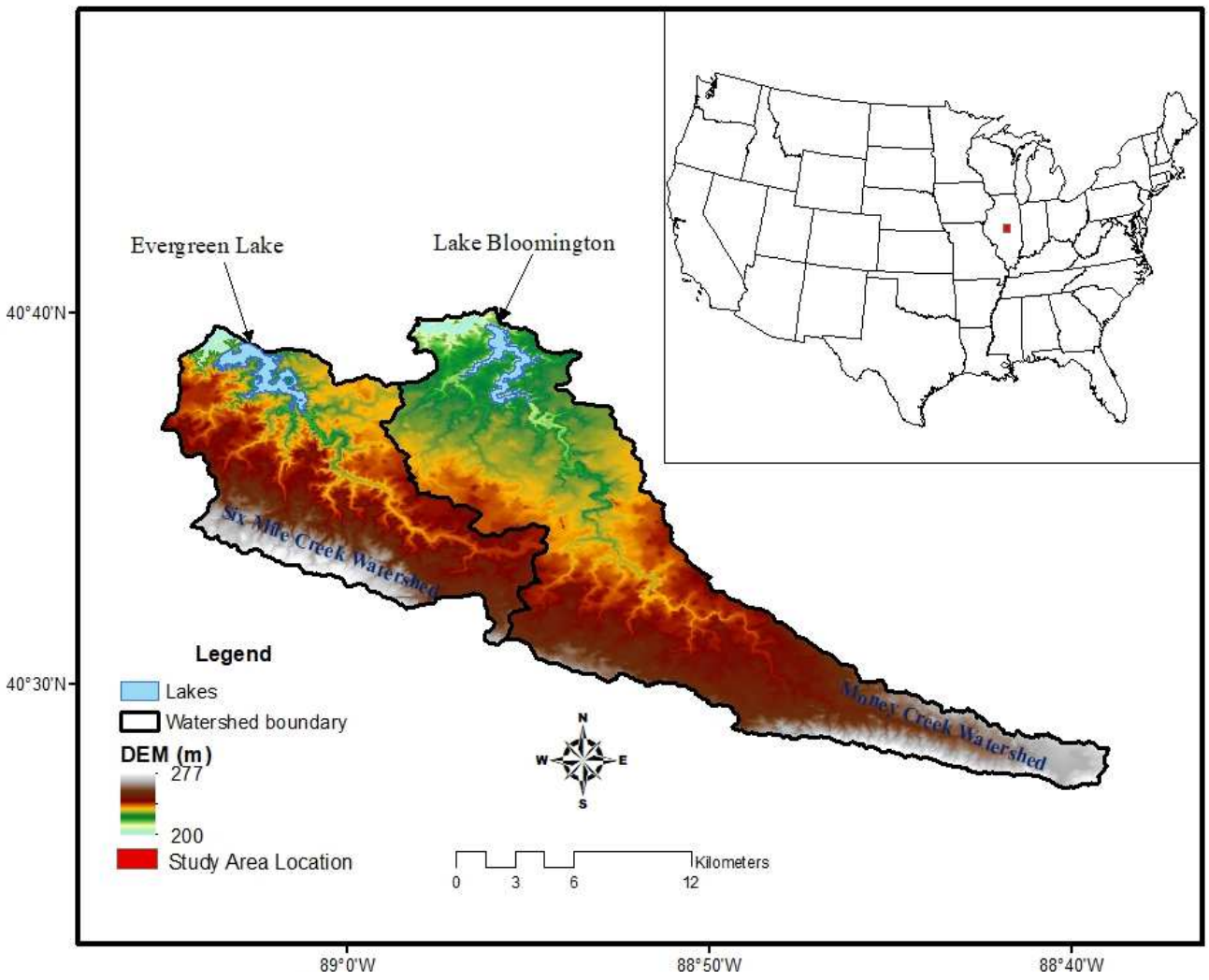

Figure 1. Location map of Lake Bloomington and Evergreen Lake.

CHAPTER III: DATA AND METHODS

This study used three approaches, (1) in-situ field sampling, (2) remote sensing, and (3) regression analysis (Figure 2), to test the conditions that influence chlorophyll *a* variability, to evaluate the usefulness of satellite imagery in detecting algal blooms in small lakes and to predict the spatial pattern of chlorophyll *a* in the study area. Lake sampling was conducted from various locations of the lakes and satellite images were downloaded from the European Satellite Agency's (ESA) Sentinel website, processed, and information was extracted. The information extracted from the images were extracted from the same locations where water samples were collected. The satellite images were processed using the ESA's Sentinel Application Platform (SNAP) software. Lastly, a regression analysis was conducted for these two data sets to test how well the satellite imagery can be used to determine algal biomass. The linear model generated was used to estimate water quality of other locations across the lake surface that were not sampled during this study.

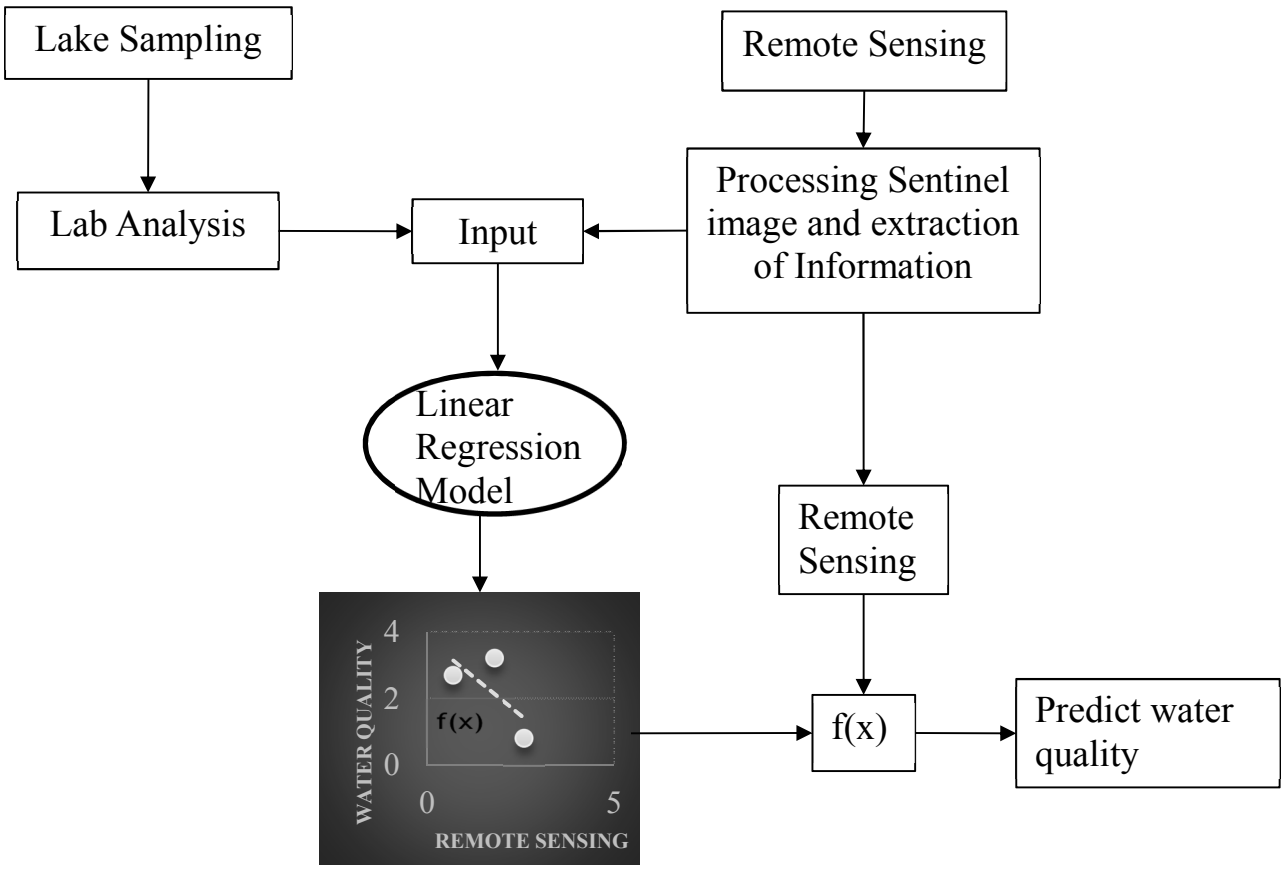

Figure 2. Flowchart of research methodology showing steps from acquisition of data from lake sampling and remote sensing to linear regression model and prediction of water quality.

Data

In-Situ Field Sampling

Four field campaigns were carried out on August 16, September 18, and October 14 of 2018 and on October 16, 2019. Field water quality tests were conducted using the EXO sonde, which is made up of a sonde with sensors and an exo handheld, and a secchi disc. The sensors can measure temperature, dissolved oxygen, conductivity, pH, chlorophyll *a* concentration and phycocyanin parameters. The sonde was connected to the handheld via Bluetooth on site and the sensor end of the sonde immersed into the water and water quality parameters were deployed to the EXO sonde. During these four sampling events, except for August 16, 2018, 19 one-liter grab

samples of surface water were collected from each location (Figure 3) to determine chlorophyll *a*, nitrate, and phosphorus concentrations. Nine samples (LB1 – LB 9), except for August 16 where only six samples were collected (LB1 – LB6), were collected from nine geolocated (Table 1) sampling locations on Lake Bloomington (Figure 4) and ten samples (EV1 – EV10) were collected from ten geolocated (Table 1**Error! Reference source not found.**) sampling locations from Evergreen Lake (Figure 3). LB 9 could not be accessed on October 16, 2019 and water was sampled from a nearby location at this date. A total of 33 samples were retrieved from Lake Bloomington and 40 samples from Evergreen Lake during the sampling period.

Table 1

Latitude and Longitude Used to Geolocate the Sampling Locations

Sample Location	Latitude	Longitude
LB 1	40.39.37	88.56.5
LB 2	40.39.23	88.55.39
LB 3	40.39.13	88.55.55
LB 4	40.38.45	88.56.3
LB 5	40.39.3	88.55.22
LB 6	40.38.47	88.55.1
LB 7	40.38.23	88.55.22
LB 8	40.37.56	88.55.42
LB 9	40.37.38	88.55.46
EV 1	40.38.43	89.3.26
EV 2	40.38.54	89.3.14
EV 3	40.39.5	89.2.48
EV 4	40.38.52	89.2.28
EV 5	40.38.33	89.2.5
EV 6	40.38.23	89.2.21
EV 7	40.38.14	89.2.10
EV 8	40.37.58	89.1.45
EV 9	40.38.21	89.1.48
EV 10	40.37.49	89.1.17

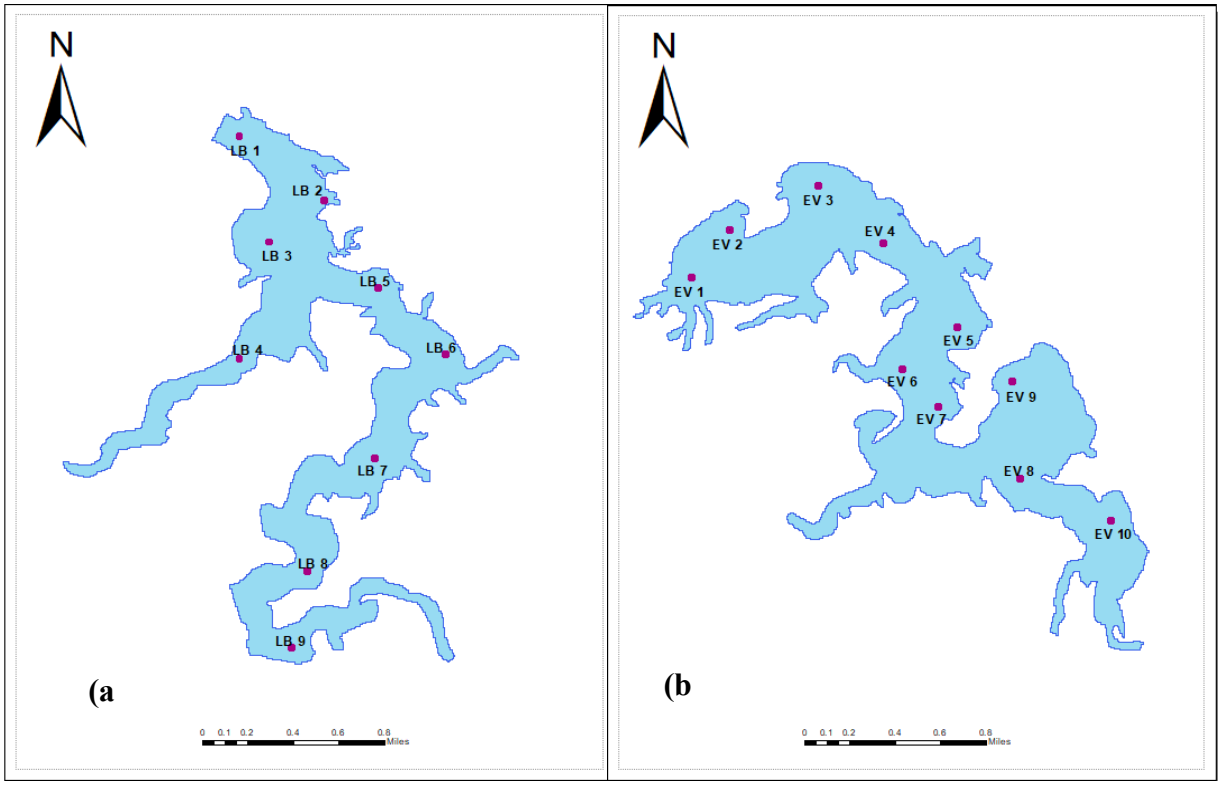

Figure 3. Sampling locations of (a) Lake Bloomington and (b) Evergreen Lake.

Remote Sensing

Satellite remote sensing images from August 19, 2018, September 23, 2018, October 16, 2018 and October 13, 2019 were downloaded from the sentinel open access hub (https://scihub.copernicus.eu/dhus/#/home, accessed on October 13, 2019). The Sentinel-2 mission option was used because it provides high resolution optical image data that supports land monitoring including soil cover, water cover, inland waterways and coastal areas. Sentinel-2 is comprised of two twin satellites S2A and S2B which carries the Multispectral Instrument (MSI) optical sensor made up of 13 bands (Table 2) with three spatial resolutions – 10m, 20m, and 60m. Bands 2, 3, 4 and 8 have a spatial resolution of 10m, bands 5, 6, 7, 8A, 11 and 12 have a spatial resolution of 20m and bands 1, 9 and 10 have a spatial resolution of 60m. The red edge bands,

Bands 5 – 7, are of interest for this study because they are useful in the estimation of chlorophyll *a* (Delegido et al., 2011).

Table 2

Sentinel-2 Bands with Wavelength and Spatial Resolutions

Band	**Band Name**	**Spectral Range (nm)**	**Resolution (m)**
1	Coastal aerosol	443	60
2	Blue	490	10
3	Green	560	10
4	Red	665	10
5	Vegetation Red Edge	705	20
6	Vegetation Red Edge	740	20
7	Vegetation Red Edge	783	20
8	Near Infrared (NIR)	842	10
8A	Vegetation Red Edge	865	20
9	Water Vapor	1360-1380	60
10	SWIR - Cirrus	10600-11190	60
11	SWIR	1610	20
12	SWIR	2190	20

Methods

Laboratory Analysis

The monochromatic method (Wetzel and Likens, 2013) was used to calculate chlorophyll *a* concentration for all samples. The water samples were filtered through a 0.45 μm glass-fiber filter and the filter placed into a labelled 15 ml centrifuge tube. Ninety percent acetone was added into the centrifuge tube which was left overnight in a freezer. Absorption rate of each sample was measured using a spectrophotometer and chlorophyll *a* concentration calculated using the following equation (Equation 1):

$$\text{Chlorophyll} - \text{a (ug/L)} = \frac{26.7 \text{ x } [(664b - 750b) - (665a - 750a)] \text{ x } volume\ of\ acetone}{Volume\ of\ sample \text{ x } l} \quad \ldots\ldots\ldots\ldots\ldots (1)$$

Where:

b is absorbance before acidification

a is absorbance after acidification

volume of acetone is the volume of 90% acetone used in the extraction (in ml)

volume of sample is the volume of water filtered (in L), and

l is the cuvette path length (cm) (typically 1cm).

For phosphorus, the Molybdate determination method of soluble reactive phosphorus was used to analyze the samples using the Genesys 10S UV-VIS spectrophotometer. A stock standard of 1 g/L P-PO_4^{3-} was diluted into a working stock solution of 5 mg/l P-PO_4^{3-}. The working stock was further diluted into four different standard concentrations in mg/L P-PO_4^{3-} (0.2, 0.5, 0.8, and 1 mg/L) in 100 ml volumetric flasks. A 0.8 ml of mixed reagent comprised of 5 N H_2SO_4, potassium antimony tartrate solution, ammonium molybdate solution, and ascorbic acid solution was added to 5 ml of the four standard concentrations in a test tube. This was also repeated for the 19 samples collected from the lakes. Absorbance of the standards and samples were read at 880 nm using the spectrophotometer. Phosphorus concentration was then calculated using the equation (Equation 2) below:

$$\text{Phosphorus (mg/L)} = \frac{\text{Absorbance} - \text{Slope}}{\text{Intercept}} \quad \ldots\ldots\ldots\ldots\ldots\ldots\ldots\ldots\ldots\ldots (2)$$

Nitrate was measured using the DIONEX ICS-1100 Ion Chromatography System and the DIONEX AS40 automated sampler. The standard method was used, and the samples were run using freshly prepared eluent solutions and three standards. The standards were used to calibrate each species of anion (chloride, fluoride, nitrate, bromide, Nitrate-N, PO_4-P and sulfate). 5ml of each stock standard was poured into a vial, covered with a vial cap and placed into a cassette from

left to right, the cassette was then inserted into the auto-sampler and then run. The same procedure was repeated for each of the lake samples, making sure there was enough eluent for the total run time.

Remote Sensing Data Processing and Algorithm

Image processing

Due to the lack of availability of cloud free images, Sentinel-2 satellite imageries were acquired from the Sentinel open access hub within ±2 to 5 days from the dates of field sampling. Before any processing of the Sentinel images, the Top-Of-Atmosphere (TOA) reflectance values were extracted from the images on SNAP. Radiation from the sun and radiation reflected from the target objects alongside the components of the atmosphere (often referred to as "atmospheric noise"), interfere with the remote sensing process to create atmospheric errors (Aggarwal, 2004) . These components of the atmosphere disperse and absorb the radiation reflected from the target objects and change its spatial distribution. Atmospheric correction of raw images downloaded is important to remove atmospheric interference in order to determine the true reflectance of the remotely sensed image. The Top-Of-Atmosphere (TOA) reflectance values are the values available after the download of the sentinel images and they are inclusive of atmospheric interference. The Sentinel images were atmospherically corrected, to remove atmospheric interference, using the Sentinel-2 Toolbox (Sen2cor v2.5.5) on SNAP. Sen2cor performs the atmospheric correction of Top-Of Atmosphere Level 1C (L1C) product to create Bottom-Of Atmosphere (BOA) Level 2A (L2A) corrected reflectance images (Muller-Wilm et al., 2013). Although other research work have classified Sen2cor as not suitable and designed for aquatic environments (Toming et al., 2016), it was used because of it was more readily available. After

the correction of the Sentinel images, information in the form of BOA reflectance values was extracted.

Remote sensing data extraction and analysis

The field sampling locations were located on the images using the GPS coordinates collected from the field. Single-pixel (1x1) extractions were conducted on the Top-Of-Atmosphere sentinel images before any atmospheric correction was done, while single-pixel (1x1) and multiple-pixel (3x3 and 5x5) extractions were conducted on the atmospherically corrected Bottom-Of-Atmosphere sentinel images. Both TOA and BOA extractions were conducted to compare their results, in order to validate the need for atmospheric correction. To extract information for the multiple pixels, resampling of the sentinel bands to 10 m was conducted because the atmospherically corrected sentinel-2 image product is a multi-sized product that contains bands of different sizes and spatial resolutions. Resampling of the images enabled the product to become a single spatial resolution image. For the multiple pixel extractions, the mean reflectance values of the combined pixels were used in all the analysis conducted.

To determine how well the satellite data could predict chlorophyll *a*, the relationship between chlorophyll *a* and three remote sensing algorithms were examined. These three remote sensing algorithms were BOA, Maximum Chlorophyll Index (MCI), and band ratios. These algorithms were tested to determine the most suitable for the lakes. For each of these algorithms, both single-pixel (1x1) and multiple-pixel (3x3 and 5x5) analysis were conducted. The multiple pixel analysis is important because it reduces noise introduced on one pixel. The BOA algorithm involved the extraction of reflectance values from the atmospherically corrected Sentinel-2 image. The band ratio algorithm involved dividing the BOA extracted reflectance value of one band by another e.g. B1/B2. Band correlation was conducted to determine which bands are highly

correlated. Bands that are highly correlated could be better predictors when used as ratios against chlorophyll *a*. The MCI algorithm, on the other hand, involves further processing of the BOA atmospherically corrected images. The MCI algorithm uses the height of the measurement in a certain spectral band above a baseline, which passes through two other spectral bands (Gower et al., 1999). The MCI algorithm on SNAP was modified from Gower's general baseline algorithm. The equation for the MCI algorithm (Equation 3) is shown below;

$$MCI = L_2 - k \text{ X } \left(\mathrm{L_1} + (\mathrm{L_3} - \mathrm{L_1}) \text{ X } \frac{\lambda_2 - \lambda_1}{\lambda_3 - \lambda_1}\right) \quad \text{(3)}$$

Where L is the water-leaving radiance computed for the Sentinel bands, centered at a wavelength λ, the indices 1 and 3 indicate the baseline bands (B4 and B6) and index 2 is the peak wavelength (B5), and k is a cloud correction constant (1.005).

Regression Analysis

After identifying the best relationship between the remote sensing algorithms and field water quality parameter, a linear regression model was fit to the data, using R, to determine the empirical relationship between chlorophyll *a* and Sentinel-2 satellite data. During the regression analysis, Sentinel-2 reflectance values were taken as the independent variable while chlorophyll *a* was considered as the dependent variable. Algorithm performance was also evaluated by using coefficient of determination (R^2), root-mean-squared error (RMSE), and probability value (p-value). The values of R^2, RMSE and p-value for all algorithms were then compared to determine the best model for chlorophyll *a* monitoring of the two lakes using Sentinel-2 satellite imagery.

CHAPTER IV: RESULTS

In Situ

Chlorophyll *a*, phosphorus, nitrate and turbidity were generally higher in Lake Bloomington than in Evergreen Lake (Table 3 and 4). Temporally, from August to October, there was generally a decreasing trend in the concentration of chlorophyll *a* for each sampling location for Lake Bloomington, except for LB 4 and LB 5 (Figure 4) which showed an increase from August to September and then decreased in October. Nitrate concentration in the lakes was generally the highest in August and lowest in September while phosphorus was generally highest in October and lowest in August and September except for LB 5, LB 8 and LB 9 (Figure 4).

Unlike Lake Bloomington, there was no seasonal trend in chlorophyll *a* concentration for Evergreen Lake. There was however a spatial pattern where chlorophyll *a* was higher upstream and lower downstream (Figure 5). Temperature showed a decreasing trend from August to October. Nitrate concentrations were too low to be detected (recorded "n.a.") for most of the sampling locations for August and September 2018 sampling campaign but were generally higher in October 2018 than October 2019 (Figure 5). For the sampling campaign on the 16th of October 2018, the concentration of phosphorus for Evergreen Lake were the same in all sampling locations except for EV 9. Phosphorus was higher in the upstream locations (EV 9 and 10) than the downstream locations (Figure 5).

Table 3

Summary of in situ Data for Lake Bloomington from the Laboratory and Exo Sonde (Field)

Water Quality Parameter	**Min**	**Max**	**Mean**	**Standard Deviation**
Chlorophyll *a* (µg/L)	2.84	150.82	50.62	29.12
Sonde chlorophyll (RFU)	1.82	12.16	4.63	2.27
BGA-PC (RFU)	0.80	6.56	3.41	1.70
Conductivity (µs/cm)	178.83	460.46	365.32	58.18
ODO (%)	58.28	201.79	110.93	40.27
ODO (mg/L)	4.74	16.44	9.99	2.90
Temp (°C)	10.04	27.46	19.96	6.06
Turbidity (FNU)	4.52	93.89	16.90	23.78
Secchi depth (cm)	14.00	70.00	46.76	14.33
Fluoride (mg/L)	0.15	2.36	0.27	0.38
Chloride (mg/L)	27.69	43.82	35.25	3.41
Bromide (mg/L)	0.12	0.13	0.12	0.01
Nitrate-N (mg/L)	0.30	1.85	0.81	0.36
PO4-P (mg/L)	0.05	0.44	0.27	0.19
Sulfate (mg/L)	7.97	51.59	17.17	6.71
Measured Phosphorus (mg/L)	0.00	0.34	0.04	0.06

Table 4

Summary of in situ Data for Evergreen Lake from the Laboratory and Exo Sonde (Field)

Water Quality Parameter	**Min**	**Max**	**Mean**	**Standard Deviation**
Chlorophyll *a* (µg/L)	1.62	82.86	34.30	17.13
Sonde chlorophyll (RFU)	0.24	6.97	3.04	1.59
BGA-PC (RFU)	0.96	3.51	1.98	0.63
Conductivity (µs/cm)	134.90	474.40	375.13	82.27
ODO (%)	64.05	469.50	121.54	63.40
ODO (mg/L)	6.16	163.75	13.75	24.40
Temp (°C)	2.96	28.64	21.21	6.78
Turbidity (FNU)	2.93	98.76	11.65	15.86
Secchi depth (cm)	15.00	120.00	53.18	23.49
Fluoride (mg/L)	0.15	0.27	0.20	0.02
Chloride (mg/L)	36.37	50.87	45.96	5.32
Bromide (mg/L)	0.11	0.13	0.12	0.01
Nitrate-N (mg/L)	0.31	1.00	0.54	0.25
PO4-P (mg/L)	-	-	-	-
Sulfate (mg/L)	12.27	23.92	16.95	2.10
Measured Phosphorus (mg/L)	0	0.07	0.01	0.01

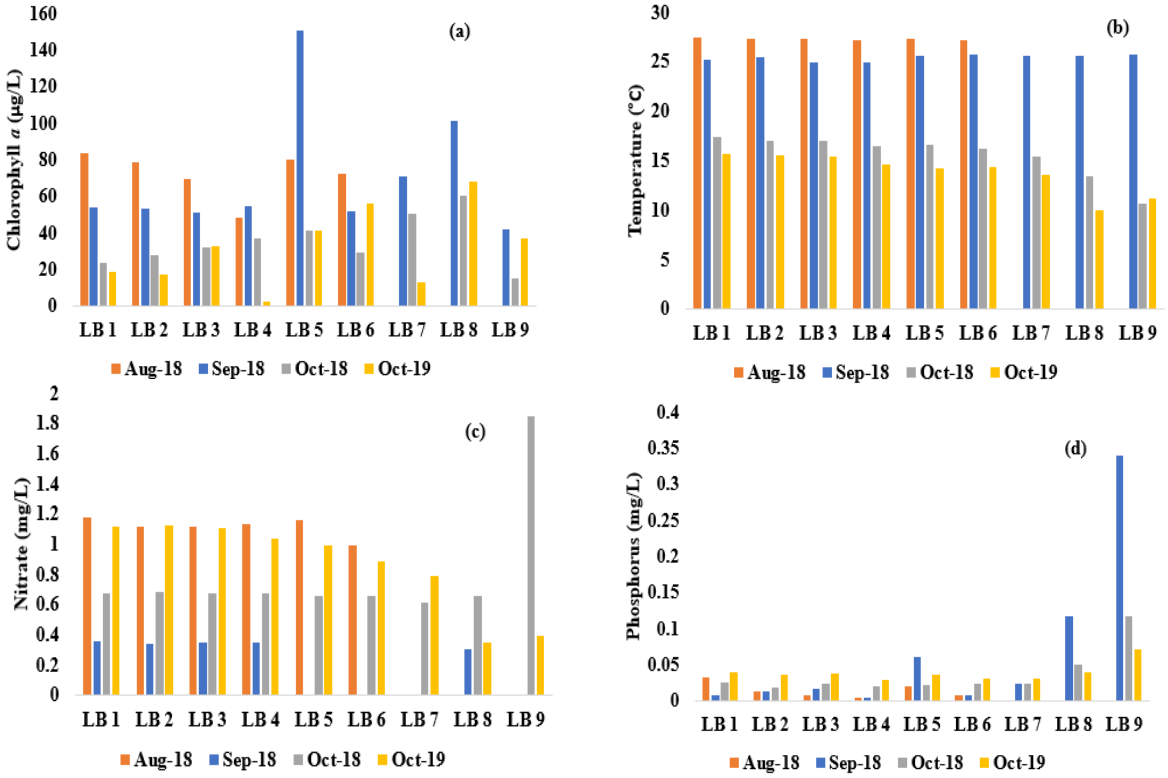

Figure 4. Temporal trend of water quality parameters for Lake Bloomington (a) chlorophyll *a*; (b) temperature; (c) nitrate; (d) phosphorus.

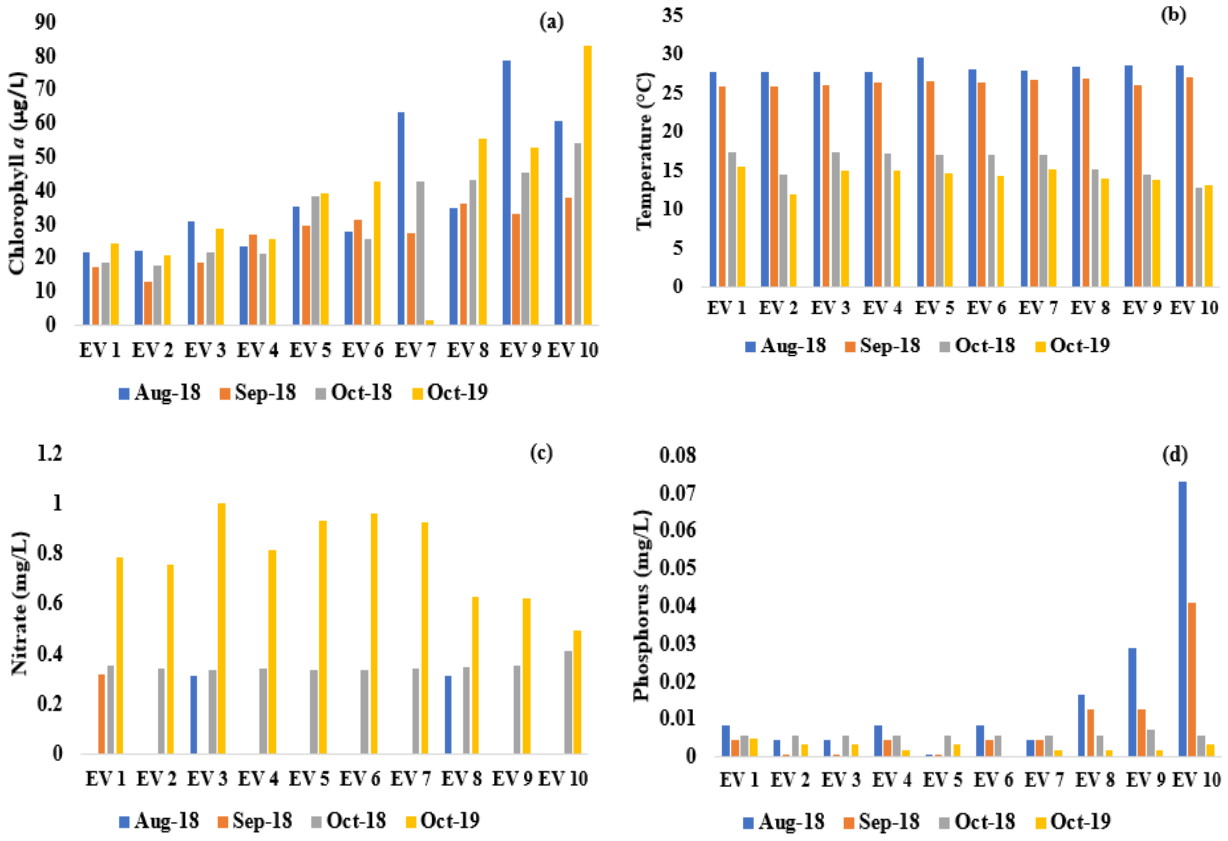

Figure 5. Temporal trend of water quality parameters for Evergreen Lake (a) chlorophyll *a*; (b) temperature; (c) nitrate; (d) phosphorus.

Turbidity was higher upstream and lower downstream for both lakes, Lake Bloomington and Evergreen Lake (Figure 6). Similar pattern was observed for phosphorus for Lake Bloomington. However, Lake Bloomington, which had a mean turbidity of 16.90FNU (Table 3), was more turbid than Evergreen Lake, which had a mean turbidity of 11.65FNU (Table 4). Secchi depth, which is a measure of the clarity of lake water, was lower in Lake Bloomington than in Evergreen Lake. This means that Evergreen Lake was clearer than Lake Bloomington, which confirms the turbidity results. Secchi depth was low upstream and high downstream for both lakes.

Except for LB 7 and EV 6, Secchi depth showed a temporal increase from August to October in 2018, while October 2018 was generally higher than October 2019 (Figure 6).

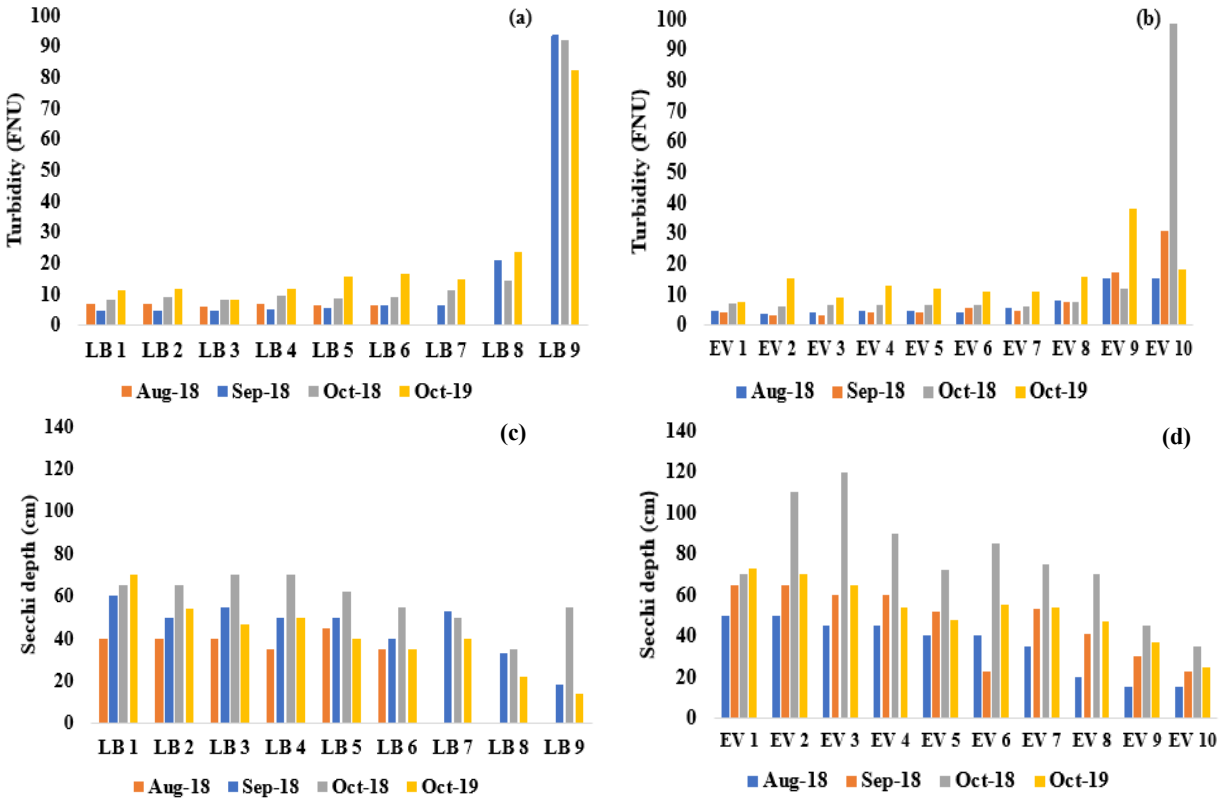

Figure 6. Turbidity and Secchi depth field data – turbidity: (a) Lake Bloomington; (b) Evergreen Lake; Secchi depth: (c) Lake Bloomington and (d) Evergreen Lake. The sample ids indicate sampling locations in space, higher id numbers (e.g. EV 10, LB 9) are upstream, while lower id numbers are downstream.

The Secchi depth pattern has an inverse relationship with chlorophyll a for Lake Bloomington (Figure 7). Temporally, as the Secchi depth increases, chlorophyll a decreased from August to October in Lake Bloomington. Turbidity also had an inverse relationship with chlorophyll a for Lake Bloomington where the less turbid the water is the higher the chlorophyll a concentration and the vice versa (Figure 7).

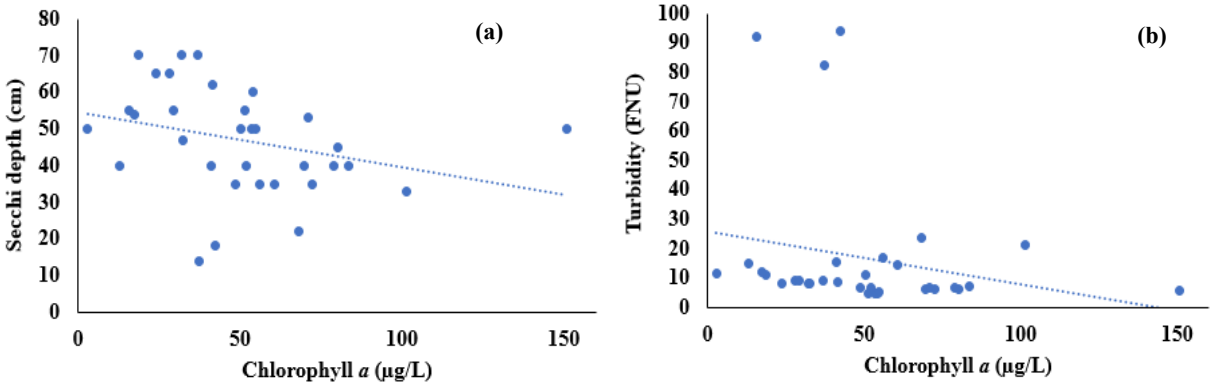

Figure 7. Chlorophyll *a* and turbidity/Secchi depth relationship for Lake Bloomington (a) Secchi depth and (b) turbidity.

Evergreen Lake showed similar relationships as Lake Bloomington between chlorophyll *a* and Secchi depth. However, there is a direct relationship between chlorophyll *a* and Turbidity (Figure 8) as opposed to that observed in Lake Bloomington. The more turbid the water, the higher the chlorophyll *a* and vice versa.

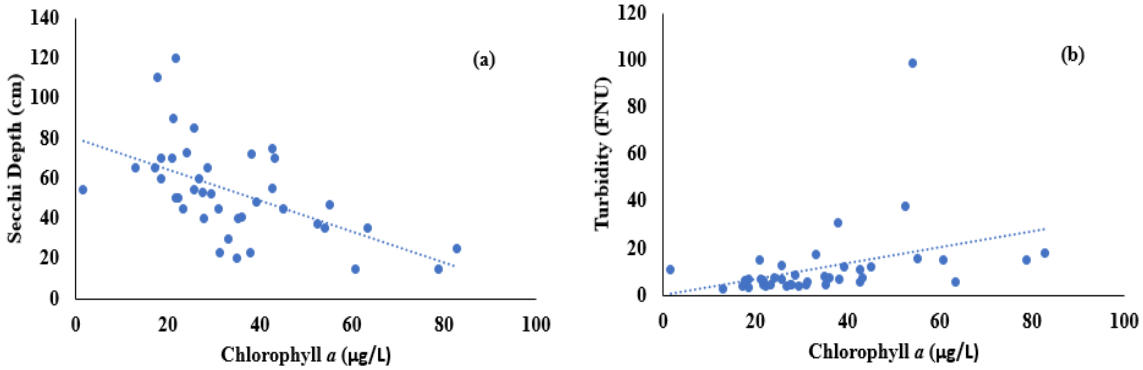

Figure 8. Chlorophyll *a* and turbidity/Secchi depth relationship for Evergreen Lake (a) Secchi depth (b) turbidity.

Satellite Remote Sensing

After the images were atmospherically corrected (Figure 9) using SNAP, band correlation was conducted for all bands and adjacent bands correlated better to each other (Chen et al., 2017). For the correlation analysis of the bands, band 10 became unavailable after atmospheric correction

was conducted for all the sentinel-2 images while band 8 became unavailable after atmospheric correction was conducted for the October 13, 2019 sentinel image. The reason for this unavailability of these bands could be because the BOA reflectance values were too low. Therefore, Bands 8 and 10 were not used for the correlation analysis between bands.

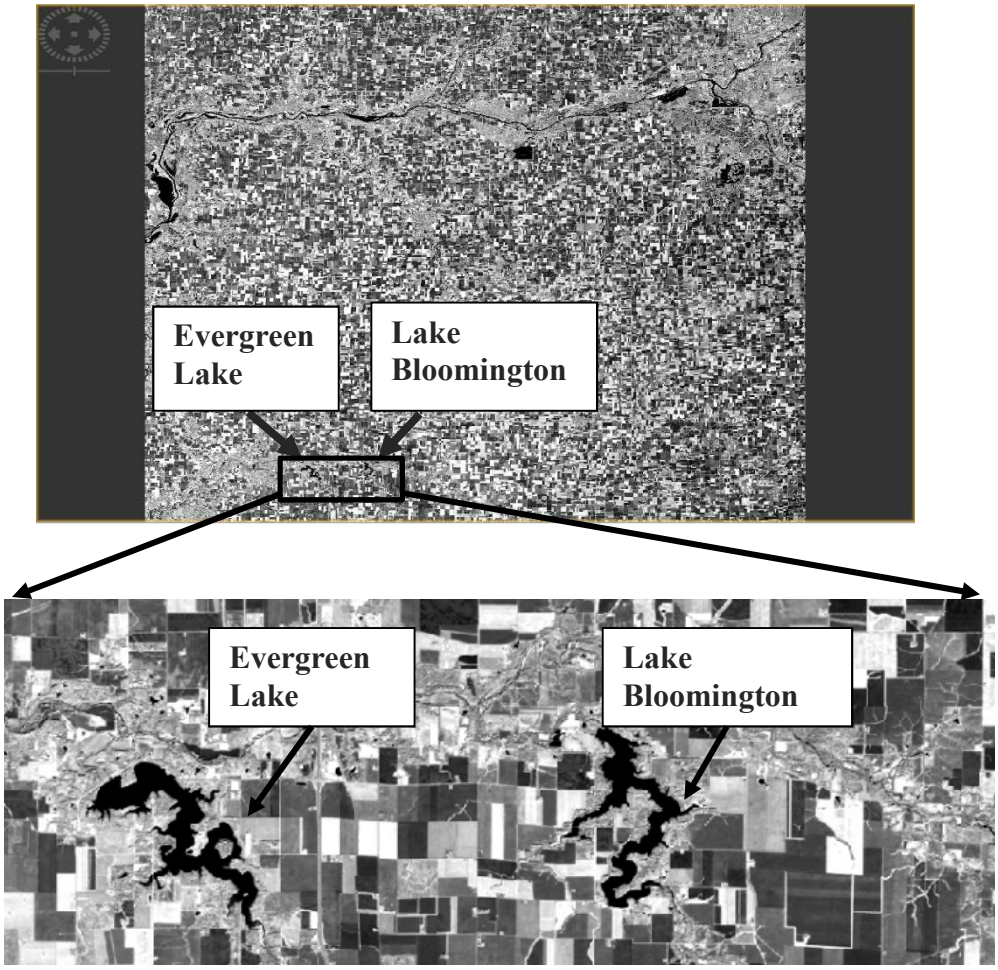

Figure 9. Atmospherically corrected sentinel image showing Lake Bloomington and Evergreen Lake.

The correlation coefficient between the bands for Evergreen Lake (Table 5) indicated that most of the bands had high correlation to their adjacent bands. For example, Band 2 is highly correlated with Band 1 and Band 3 which are adjacent to it and Band 4 is highly correlated with Bands 3 and 5 which are adjacent to it. However, some bands did not have a high correlation with

adjacent bands. For example, Band 6 correlated highly with Bands 1 and 2 in contrast to Bands 5 and 6 which are its adjacent bands, while Bands 11 and 12 had no strong correlation with any band.

Table 5

Correlation Coefficient (r) Values of Sentinel-2 Bands for Evergreen Lake (Single Pixel)

Band No	**Band 1**	**Band 2**	**Band 3**	**Band 4**	**Band 5**	**Band 6**	**Band 7**	**Band 8A**	**Band 9**	**Band 11**
Band 1	—	—	—	—	—	—	—	—	—	—
Band 2	**0.94**	—	—	—	—	—	—	—	—	—
Band 3	0.86	**0.92**	—	—	—	—	—	—	—	—
Band 4	0.69	0.80	**0.91**	—	—	—	—	—	—	—
Band 5	0.62	0.71	0.86	**0.94**	—	—	—	—	—	—
Band 6	0.90	0.96	0.94	0.84	0.82	—	—	—	—	—
Band 7	0.91	0.96	0.93	0.83	0.79	**1.00**	—	—	—	—
Band 8A	0.88	0.93	0.89	0.77	0.75	**0.98**	**0.98**	—	—	—
Band 9	0.93	0.94	0.86	0.67	0.61	0.94	**0.94**	**0.93**	—	—
Band 11	0.50	0.59	0.52	0.54	0.46	0.61	0.63	0.67	0.59	—
Band 12	0.26	0.24	0.25	0.18	0.17	0.32	0.33	0.32	0.36	0.20

Note. High correlation values are highlighted in bold.

The correlation coefficients between the bands also indicated that most adjacent bands are highly correlated for Lake Bloomington. For example, Band 2 is highly correlated with Band 1 and Band 3 which are adjacent to it, and Band 4 highly correlated with Band 3 and 5 which are adjacent to it (Table 6). There were also some bands that did not have a strong correlation with any bands i.e. bands 6, 7, and 11.

Table 6

Correlation Coefficient (r) Values of Sentinel-2 Bands for Lake Bloomington (Single Pixel)

Band No	Band 1	Band 2	Band 3	Band 4	Band 5	Band 6	Band 7	Band 8A	Band 9	Band 11
Band 1	—	—	—	—	—	—	—	—	—	—
Band 2	**0.88**	—	—	—	—	—	—	—	—	—
Band 3	0.61	**0.84**	—	—	—	—	—	—	—	—
Band 4	0.25	0.60	**0.88**	—	—	—	—	—	—	—
Band 5	0.37	0.63	0.85	**0.90**	—	—	—	—	—	—
Band 6	0.81	0.93	0.85	0.69	0.79	—	—	—	—	—
Band 7	0.81	0.91	0.80	0.64	0.74	**0.99**	—	—	—	—
Band 8A	0.78	0.89	0.74	0.6	0.66	**0.95**	**0.97**	—	—	—
Band 9	0.73	0.56	0.38	0.16	0.22	0.55	0.60	0.60	—	—
Band 11	0.20	0.22	0.11	0.20	0.15	0.30	0.37	0.49	0.41	—
Band 12	0.10	0.13	0.07	0.21	0.09	0.20	0.25	0.36	0.36	**0.87**

Note. Top row bands are divided by side column bands. High correlation values are highlighted in bold.

Bottom-Of-Atmosphere (BOA) Vs Top-Of-Atmosphere Reflectance (TOA)

This comparison was done using the 1x1 pixel reflectance extracted from the satellite imageries. The purpose is to compare the relationship between TOA and BOA values with chlorophyll *a* and choose the optimum approach.

Lake Bloomington

When plotted against chlorophyll *a* after the atmospheric correction (conversion of TOA to BOA) was conducted using SNAP, there was mostly a decline in the correlation coefficient (r) values for Lake Bloomington (Table 7). Improvement was observed only in bands 1,4, 9, and 12, with the greatest percentage increase in band 12 which has a 900% increase from 0.03 to 0.30 in correlation (Table 7). However, most of the correlation coefficients were very insignificant with the most significant correlation coefficient observed in band 1, which increased from TOA correlation coefficient of 0.22 to BOA correlation coefficient of 0.36.

Evergreen Lake

Except for bands 1 and 12 which had a decline of 17% and 86% respectively, there was generally an improvement in the correlation coefficients from TOA to BOA for Evergreen Lake. The greatest percentage increase was observed in band 2 which had a 227% increase from 0.11 to 0.36 (Table 7), but the highest correlation coefficient value was observed in band 5 with an 18% increase from 0.56 to 0.66 (Table 7).

Overall, the relationship between the BOA reflectance and chlorophyll *a* showed higher correlation coefficient than the TOA reflectance for both Lake Bloomington and Evergreen, and as such, the BOA reflectance was used for all subsequent analyses.

Table 7

Cross Relationship Between Chlorophyll a and TOA and BOA Atmospheric Correction for Lake Bloomington and Evergreen Lake

Lake Bloomington				**Evergreen Lake**			
Bands	**TOA**	**BOA**	**% Change**	**TOA**	**BOA**	**% Change**	**Bands**
Band 1	0.22	0.36	64	0.30	0.25	-17	Band 1
Band 2	0.17	0.12	-29	0.11	0.36	227	Band 2
Band 3	0.10	0.05	-50	0.38	0.48	26	Band 3
Band 4	0.03	0.28	833	0.44	0.55	25	Band 4
Band 5	0.05	0.04	-20	0.56	0.66	18	Band 5
Band 6	0.26	0.10	-62	0.30	0.48	60	Band 6
Band 7	0.28	0.11	-61	0.30	0.45	50	Band 7
Band 8	0.27	0.19	-30	0.30	-	-	Band 8
Band 8A	0.28	-	-	0.17	0.45	165	Band 8A
Band 9	0.12	0.24	100	0.28	0.30	7	Band 9
Band 10	0.11	-	-	0.26	-	-	Band 10
Band 11	0.20	0.09	-55	0.22	0.28	27	Band 11
Band 12	0.03	0.30	900	0.28	0.04	-86	Band 12

Note. Comparison of TOA and BOA reflectance with chlorophyll a was conducted with only the 1x1 pixel analysis and the numbers represent r values.

Chlorophyll *a* Vs Remote Sensing Algorithms

The measured concentrations of chlorophyll *a* for all sampling events were plotted against reflectance values from the three algorithms. 1x1, 3x3 and 5x5 pixel analyses were conducted for all three remote sensing algorithms. Extraction of MCI values for the August 19, 2018 image could not be conducted because the lakes were not detected after processing for MCI (Figure 10). This prompted the MCI analysis to be carried out without including MCI values from the August 2018 image. For the Band ratio Algorithm, only two-band ratio models (2-B models) were tested because the 2-B models are simple and enough to not introduce uncertainty factors that additional wavelengths would (Zhu et al., 2014). All possible 2-B combination for single and multiple pixel analysis was tested using bands 1-7 since they can readily detect algae.

A comparison of the best results from all three algorithms was conducted to show the algorithms with the highest correlation with chlorophyll *a*. This was important because the best algorithm was chosen and used for the regression analysis conducted.

Figure 10. MCI images showing Lake Bloomington and Evergreen Lake (a) September 23, 2018 image (b) August 19, 2019 image. White color indicates areas covered with water while black indicates areas without water.

Lake Bloomington

Bottom of Atmosphere Algorithm

Lake Bloomington showed poor correlation between chlorophyll *a* and all the band reflectance for both single-pixel and multiple pixels analysis. The correlation coefficients for Lake Bloomington ranged from 0.05 to 0.36 for the single pixel analysis, 0.01 to 0.33 for the 3x3-pixel analysis, and from 0.01 to 0.35 for the 5x5-pixel analysis (Table 8). The highest correlation was observed between band 1 and chlorophyll *a* for all pixel analyses. For band 1, 1x1-pixel analysis had a correlation coefficient of 0.36, 3x3-pixel analysis had a correlation coefficient of 0.33, while 5x5-pixel analysis had a correlation coefficient of 0.35. Except for Bands 3, 5 and 11, the 1x1-pixel analysis showed higher correlation coefficients than both 3x3- and 5x5- pixel analyses.

Maximum Chlorophyll Index (MCI) Algorithm

The MCI for Lake Bloomington showed no significant correlation with the measured chlorophyll *a* for all pixel analyses (Table 8). The highest correlation coefficient of 0.16 was observed in the 3x3-pixel analysis.

Table 8

BOA and MCI Cross Relationship (r values) for Lake Bloomington

Bands	**Single-Pixel**	**3x3-Pixel**	**5x5-Pixel**
Band 1	0.36	0.33	0.35
Band 2	0.12	0.10	0.10
Band 3	0.05	0.06	0.04
Band 4	0.28	0.24	0.23
Band 5	0.04	0.05	0.05
Band 6	0.10	0.07	0.07
Band 7	0.11	0.07	0.07
Band 8	-	-	-
Band 8A	0.05	0.01	0.01
Band 9	0.24	0.22	0.20
Band 10	-	-	-
Band 11	0.09	0.12	0.14
Band 12	0.30	0.22	0.24
MCI	0.09	0.16	0.14

Note. Analysis is between chlorophyll a and BOA/MCI algorithms.

Band Ratio Algorithm

For Lake Bloomington, the 1x1 pixel analysis produced greater correlation coefficients except for B1/B2, B1/B6, B1/B7, B3/B5, B6/1 and B7/B1 (Tables 9, 10 and 11). The highest correlation coefficient was observed in B1/B2 in all the pixel analyses, but it was highest in the 5x5-pixel analysis with a 0.55 correlation coefficient.

Table 9

Cross Relationship (r values) Between Chlorophyll a and 2-B Ratio for Lake Bloomington (Single Pixel)

Band No	Band 1	Band 2	Band 3	Band 4	Band 5	Band 6	Band 7
Band 1	—	**0.51**	0.42	0.45	0.35	0.34	0.31
Band 2	**0.47**	—	0.23	0.36	0.13	0	0.03
Band 3	**0.49**	0.24	—	**0.49**	0.03	0.12	0.13
Band 4	**0.51**	0.37	**0.50**	—	0.44	0.23	0.23
Band 5	0.45	0.23	0.01	**0.46**	—	0.15	0.15
Band 6	0.28	0.04	0.09	0.21	0.07	—	0.08
Band 7	0.29	0.29	0.12	0.22	0.11	0.09	—

Note. Top row bands divided by side column bands (highest values are highlighted in bold).

Table 10

Cross Relationship (r values) Between Chlorophyll a and 2-B Ratio for Lake Bloomington (3x3 Pixel)

Band No	Band 1	Band 2	Band 3	Band 4	Band 5	Band 6	Band 7
Band 1	—	**0.50**	0.41	0.43	0.35	0.34	0.33
Band 2	**0.52**	—	0.18	0.31	0.09	0	0.01
Band 3	**0.47**	0.19	—	0.35	0.01	0.08	0.09
Band 4	**0.49**	0.32	0.39	—	0.38	0.20	0.20
Band 5	0.44	0.19	0	0.40	—	0.13	0.13
Band 6	0.10	0	0.09	0.19	0.07	—	0.07
Band 7	0.32	0.04	0.12	0.21	0.10	0.09	—

Note. Top row bands divided by side column bands (highest values are highlighted in bold).

Table 11

Cross Relationship (r values) Between Chlorophyll a and 2-B Ratio for Lake Bloomington (5x5 Pixel)

Band No	Band 1	Band 2	Band 3	Band 4	Band 5	Band 6	Band 7
Band 1	—	**0.52**	0.41	0.43	0.36	0.36	0.35
Band 2	**0.55**	—	0.16	0.31	0.09	0	0.01
Band 3	**0.47**	0.17	—	0.38	0.01	0.07	0.07
Band 4	**0.49**	0.32	0.42	—	0.38	0.20	0.19
Band 5	0.45	0.18	0.03	0.41	—	0.13	0.12
Band 6	0.31	0	0.08	0.19	0.07	—	0.06
Band 7	0.33	0.04	0.11	0.20	0.10	0.08	—

Note. Top row bands divided by side column bands (highest values are highlighted in bold).

Based on the results above, the best result for the BOA algorithm was in the 1x1-pixel analysis for Band 1 with a correlation coefficient of 0.36. The best result for the MCI algorithm was the 3x3-pixel analysis which showed a correlation coefficient of 0.16. The band ratio was in the 5x5-pixel analysis for B1/B2 which showed a correlation coefficient of 0.55. Overall, the best result for the band ratio produced the best results for Lake Bloomington.

Evergreen Lake

Bottom of Atmosphere Algorithm

Evergreen Lake showed a stronger correlation than Lake Bloomington between chlorophyll *a* and the bands of the BOA algorithm for all pixel analyses. The correlation coefficients for Evergreen Lake ranged from 0.04 to 0.66 for the single-pixel analysis, from 0.20 to 0.66 for 3x3-pixel analysis and from 0.12 to 0.66 for 5x5-pixel analysis (Table 12). The highest correlation was observed in band 5 for all pixel analyses. For band 5, all pixel analyses showed a correlation coefficient of 0.66.

Maximum Chlorophyll Index (MCI) Algorithm

The MCI for Evergreen Lake showed significant correlation with measured chlorophyll *a* for both the single and multiple pixel analyses (Table 12). The highest correlation of 0.69 was observed in the 5x5- pixel analysis.

Table 12

BOA and MCI Cross Relationship (r values) for Evergreen Lake

Bands	**Single-Pixel**	**3x3-Pixel**	**5x5-Pixel**
Band 1	0.25	0.24	0.24
Band 2	0.36	0.37	0.37
Band 3	0.48	0.48	0.48
Band 4	0.55	0.57	0.57
Band 5	0.66	0.66	0.66
Band 6	0.48	0.47	0.47
Band 7	0.45	0.45	0.45
Band 8	-	-	-
Band 8A	0.45	0.45	0.46
Band 9	0.30	0.28	0.27
Band 10	-	-	-
Band 11	0.28	0.29	0.30
Band 12	0.04	0.20	0.12
MCI	0.68	0.67	0.69

Note. Analysis is between chlorophyll a and BOA/MCI algorithms.

Band Ratio Algorithms

For Evergreen Lake, the multiple pixel analyses (3x3 and 5x5) produced greater correlation coefficients than the single-pixel analysis with the highest overall correlation in the 5x5-pixel analysis (Tables 13, 14 and 15). The highest correlation coefficient was observed in B5/B4 in all the pixel analyses, but it was highest in the 3x3- and 5x5-pixel analysis with a 0.69 correlation coefficient.

Table 13

Cross Relationship (r values) Between Chlorophyll a and 2-B Ratio for Evergreen Lake (Single Pixel)

Band No	Band 1	Band 2	Band 3	Band 4	Band 5	Band 6	Band 7
Band 1	—	0.04	0.11	0.02	0.23	**0.59**	**0.59**
Band 2	0.06	—	0.16	0.04	0.39	0.58	0.52
Band 3	0.05	0.13	—	0.31	**0.64**	0.47	0.43
Band 4	0.06	0.04	0.33	—	**0.64**	0.39	0.35
Band 5	0.26	0.38	**0.62**	**0.60**	—	0.25	0.21
Band 6	0.38	0.47	0.41	0.42	0.33	—	0.17
Band 7	0.47	0.38	0.35	0.32	0.24	0.03	—

Note: *Top row bands divided by side column bands (highest values are highlighted in bold).*

Table 14

Cross Relationship (r values) Between Chlorophyll a and 2-B Ratio for Evergreen Lake (3x3 Pixel)

Band No	Band 1	Band 2	Band 3	Band 4	Band 5	Band 6	Band 7
Band 1	—	0	0.09	0.05	0.24	**0.60**	**0.60**
Band 2	0.06	—	0.19	0.04	0.40	0.57	0.53
Band 3	0.04	0.15	—	0.34	**0.63**	0.46	0.43
Band 4	0.08	0.06	0.36	—	**0.69**	0.36	0.35
Band 5	0.26	0.40	**0.61**	**0.66**	—	0.26	0.23
Band 6	0.44	0.49	0.45	0.43	0.36	—	0.21
Band 7	0.49	0.41	0.38	0.34	0.27	0.09	—

Note: *Top row bands divided by side column bands (highest values are highlighted in bold).*

Table 15

Cross Relationship (r values) Between Chlorophyll a and 2-B Ratio for Evergreen Lake (5x5 Pixel)

Band No	Band 1	Band 2	Band 3	Band 4	Band 5	Band 6	Band 7
Band 1	—	0	0.08	0.01	0.24	**0.60**	**0.61**
Band 2	0.07	—	0.18	0.05	0.40	0.56	0.52
Band 3	0.03	0.15	—	0.34	**0.63**	0.46	0.43
Band 4	0.08	0.06	0.36	—	**0.69**	0.38	0.35
Band 5	0.26	0.40	**0.62**	**0.67**	—	0.25	0.22
Band 6	0.46	0.50	0.45	0.43	0.35	—	0.18
Band 7	0.49	0.44	0.40	0.36	0.28	0.09	—

Note. Top row bands divided by side column bands (highest values are highlighted in bold).

Based on the results above, the best result for the BOA algorithm was observed in band 5 with all pixel analyses having the same correlation coefficient of 0.66. The best result for the MCI algorithm was the 5x5-pixel analysis which showed a correlation coefficient of 0.69. The best result for the band ratio was in the 3x3- and 5x5-pixel analyses for B5/B4 which showed a correlation coefficient of 0.69. Overall, the MCI and band ratio produced the best results for Evergreen.

Regression Analysis

Lake Bloomington

The satellite reflectance data for Lake Bloomington showed weak relationships with chlorophyll *a* for the algorithms tested. A comparison of each field sampling event (August – October) and their corresponding satellite data was conducted using the 5x5-pixel reflectance values for Lake Bloomington. The strongest relationship was observed in Band 5 and B1/B2 ratio (Table 16) but the band ratio was used for used for the regression analysis. The results of the regression analysis (Table 17) showed that the relationships between the field and satellite data

were statistically insignificant (p-value>0.05). The relationships observed in Lake Bloomington were not strong enough or statistically significant to perform further analysis.

Table 16

Cross Relationship for Individual Sampling Events for Lake Bloomington

Month and Year	Band 5	B1/B2	MCI
August 2018	0.24	0.32	-
September 2018	0.0005	0.04	0.005
October 2018	0.62	0.0007	0.80
October 2019	0.04	0.27	0.10

Note: Correlation coefficient (r) values between chlorophyll a and satellite data for individual sampling.

Table 17

Regression Analysis for Lake Bloomington between B1/B2 and Chlorophyll a for Individual Month

Month and Year	Slope	p-value	Intercept	p-value	R^2	p-value
Aug-2018	250.4	0.238	-108.1	0.453	0.324	0.238
Sep-2018	-111.7	0.59	149.5	0.324	0.044	0.59
Oct-2018	-4.569	0.944	37.37	0.22	0.0007	0.944
Oct-2019	-493.7	0.114	266.9	0.114	0.266	0.1557

Evergreen Lake

The satellite reflectance data for Evergreen lake showed stronger relationships with chlorophyll *a* for each of the algorithms tested. A comparison of each field sampling event (August – October) and their corresponding satellite data was conducted using the 5x5-pixel reflectance values for Evergreen Lake. For the BOA reflectance and band ratio algorithms, a stronger relationship was observed in Band 5 and B5/B4 ratio respectively (Table 18) and these were used

for the regression analysis. The highest correlation coefficient for the months was observed as follows; Band 5 for August 2018 with a correlation coefficient of 0.68 and R^2 of 0.46, band ratio B5/B4 for September 2018 with a correlation coefficient of 0.80 and R^2 of 0.64, MCI for October 2018 with a correlation coefficient of 0.97 and R^2 of 0.94 and band ratio B5/B4 for October 2019 with a correlation coefficient of 0.75 and R^2 of 0.56 (Figure 11). Data from October 2018 showed the highest correlation values compared to all the other months.

Table 18

Cross Relationship for Individual Sampling Events for Evergreen Lake

Month and Year	Band 5	B5/B4	MCI
August 2018	0.68	0.58	-
September 2018	0.73	0.80	0.73
October 2018	0.94	0.93	0.97
October 2019	0.71	0.75	0.74

Note. Correlation coefficient (r) values between chlorophyll a and satellite data for individual sampling.

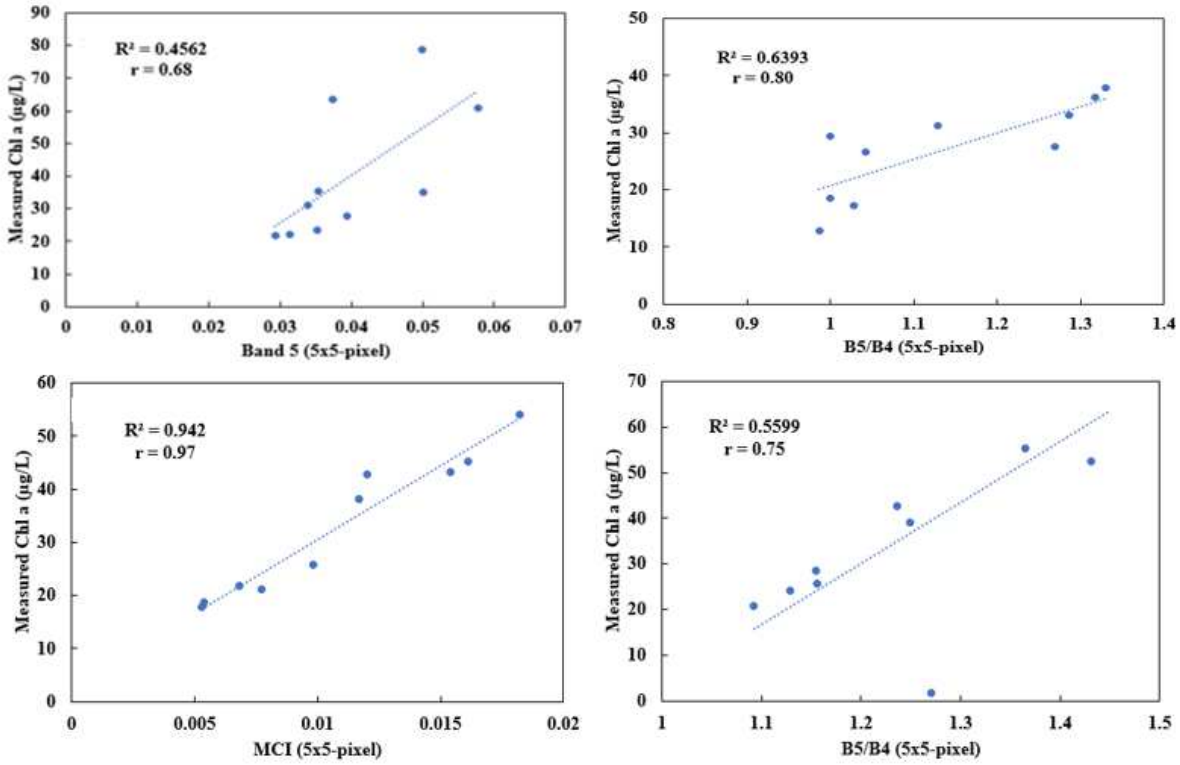

Figure 11. Scatter plot of the best results of the regression analysis for Evergreen Lake between chlorophyll *a* and remote sensing algorithms for individual months (a) August 2018 (b) September 2018 (c) October 2018 (d) October 2019.

To estimate spatial variation of chlorophyll *a* for Evergreen Lake, a linear regression model was fit to the data. The result of the comparison of band ratio (B5/B4) and chlorophyll *a* was used for this estimation for individual sampling events. The results showed that the August 2018 model was not statistically significant because the p-values for each variable tested was greater than 0.05 (p-value>0.05). However, the other sampling events were statistically significant with p-values <0.05 for each variable tested, and October 2018 having the highest R^2 of 0.87 (Table 19).

Table 19

Regression Analysis for Evergreen Lake Between B5/B4 and Chlorophyll a for Individual Month

Month and Year	Slope	p-value	Intercept	p-value	R^2	p-value
Aug-2018	108.87	0.08	-94.47	0.19	0.34	0.077
Sep-2018	46.09	0.01	-25.44	0.11	0.64	0.006
Oct-2018	68.53	8.80E-05	-44.4	0.0033	0.87	8.80E-05
Oct-2019	133.7	0.013	-130.21	0.039	0.56	0.013

The results of the regression analysis were used as inputs for the creation of interpolated spatial maps that show the spatial distribution of chlorophyll *a* in Evergreen Lake.

CHAPTER V: DISCUSSION

What Factors Influence the Distribution of Chlorophyll *a*?

Lake Bloomington

The seasonal trend displayed by chlorophyll *a* in Lake Bloomington is evidently influenced by the observed seasonal changes in temperature, as the lake water temperature decrease from August to October. The higher the temperature, the higher the concentration of chlorophyll *a* which translates to a higher number of algae in the summer than in fall. Nutrients, on the other hand, do not have a consistent seasonal or spatial pattern. Phosphorus was higher upstream and lower at downstream sampling locations while nitrate was higher downstream and decreases upstream. The higher concentration of phosphorus observed upstream could be due to the presence of more sediments upstream than downstream. Sediments play an important role in phosphorus metabolism because they are able to retain and release phosphorus in lakes (Pettersson, 1998). The higher concentration of nitrate downstream could be because it is a water-soluble nutrient and is readily transported due to its high solubility and mobility characteristics (Vesper et al., 2001). Lake Bloomington was more turbid upstream than downstream and secchi depth was low upstream and high downstream. For Lake Bloomington, the clearer the water, the lower concentration of chlorophyll *a* and vice versa. One would expect more turbid waters to have higher concentrations of chlorophyll *a*, and vice versa, but this was not the case. The inverse relationship observed between turbidity and chlorophyll *a* could be because sediment load contributed to Lake Bloomington's turbidity more than algae. This sediment load could interfere with the satellite and make it more difficult for the detection of chlorophyll *a* in the more turbid waters.

Evergreen Lake

The seasonal increase in nitrate observed for Evergreen Lake could be because farmers apply fertilizers before the growing season in April/May and after harvest in October/November. Because of its high solubility and mobility, nitrate is easily dissolved and leached from the ground which would explain why most of the August and September 2018 nitrate were too low to be detected. Another reason for the low detection of nitrate could be because there was no water flow into the fields from streams or tiles. Another technique for measuring and estimating nitrate can be employed given that the lake levels were usually high during the sampling periods. The temporal increase observed in October 2019 when compared to October 2018 could be due to the types of crops grown each year. Farmers would generally apply more fertilizers when corn is dominantly grown and less fertilizers when soybeans is dominantly grown. Phosphorus showed no temporal changes but spatially seems to be high upstream and lower downstream. This spatial pattern of phosphorus, like in Lake Bloomington, can also be attributed to the presence of more sediments upstream than downstream. The seasonal pattern observed in chlorophyll *a* is influenced by the concentration of Phosphorus as the higher the concentration of phosphorus, the higher the chlorophyll *a* concentration and the lower the phosphorus, the lower the chlorophyll *a*. The direct relationship between turbidity and chlorophyll *a* in Evergreen Lake could be because algae rather than sediment load contributed more to the turbidity of the lake.

How Well Does the Satellite Imagery Capture Chlorophyll *a*?

The results from the remote sensing analysis showed there was no significant relationship between chlorophyll *a* and the sentinel algorithms after atmospheric correction was conducted for Lake Bloomington. Except for band ratio Band1/Band2 (B1/B2), which had a correlation coefficient of 0.55 and an R^2 value of 0.31 for a 5x5-pixel averaging window, the relationships observed were very weak. Weak relationship between chlorophyll *a* and the satellite algorithms could be because of the interference of turbidity with the satellite on Lake Bloomington. Even though there are algae present in Lake Bloomington as evidenced by the measured chlorophyll *a* values, the turbidity might be inducing noise on the reflectance values recorded by the satellite. When different zones of the lakes were analyzed, the deep-water zone (LB1 – LB4) showed a general improvement in the correlation coefficients with the highest correlation coefficient of 0.74 and an R^2 of 0.56 observed in Band 4. Small lakes can easily become turbid with large influx of sediment load into the lake. This better correlation results observed in the less turbid portions of the lake shows that remote sensing data can be used to predict chlorophyll *a* concentrations in lakes with low turbidity but is difficult in reservoirs with high turbidity rates. Previous studies suggested that atmospheric correction might not be required for the estimation of chlorophyll *a*, in small turbid waterbodies (Matthews et al., 2010).

The relationship observed in Evergreen Lake were stronger and more significant than those of Lake Bloomington. This could be because Evergreen Lake is bigger and less turbid than Lake Bloomington. This could also be because algae contributed more to the turbidity of the lake than sediment load, reducing the interference of sediment load with the reflectance recorded by the satellite. After atmospheric correction was conducted to convert TOA to BOA, there was improvement in the relationships between chlorophyll *a* and the reflectance values. Therefore,

atmospherically corrected images can be used in the analysis of the less turbid and bigger Evergreen Lake. The most significant relationships were observed in band 5 for the BOA algorithm, band ratio B5/B4 for the two-band ratio algorithm and in the MCI algorithm for Evergreen Lake. For the analysis of the individual sampling events, October 2018 recorded the highest correlation coefficient for BOA, MCI and band ratio. The time window between field sampling and collection of data by the satellite is within ±2 days for October 2018 as opposed to ±3-5 days for the other three sampling events. This means that remote sensing analysis for chlorophyll *a* should be limited to a time window of ±2 days, because the October 2018 sampling event was within ±2 days and the other sampling events were within ±3-5 days.

The satellite imagery was a better predictor of chlorophyll *a* for Evergreen Lake than Lake Bloomington. As stated earlier, this could be as a result of the high turbidity of Lake Bloomington, contributed by sediment load rather than algae. Due to weather conditions and the availability of cloud free images, there were limited sampling events (only four) and lack of sampling events that coincided with satellite overpass time for this project. This could also be a reason for the regression results observed in the two lakes. Previous studies have shown that when predicting chlorophyll *a* using satellites, the time window between field sampling and satellite image acquisition should be limited to ±2 days (Stadelmann et al., 2001). Frequent sampling of the lakes, e.g. every two weeks or once a month, could help reduce errors and produce better results with the satellite data. Better remote sensing atmospheric correction methods and algorithms could also be tested out on the lakes to see if there would be any improvements. The traditional empirical line method (ELM) has been used over the Sen2Cor tool on SNAP (Ha et al., 2017) because it is a more precise method for atmospheric correction over water areas. The slope model (SLMSI) and Normalized Difference Chlorophyll Index (NDCI) algorithms (Watanabe et al., 2018) developed for turbid waters have

also been successfully used in the prediction of chlorophyll *a* concentrations using satellite imagery. These atmospheric correction methods and algorithms can be applied to and tested on Lake Bloomington and Evergreen lake.

What is the Spatial Pattern of Chlorophyll *a* in the Lakes?

Since the satellite imagery captured chlorophyll *a* better in Evergreen Lake, the spatial pattern analysis was conducted for Evergreen Lake only. Maps showing the spatial pattern of chlorophyll *a* in Evergreen Lake were created for each sampling event (Figure 12) using pixel values from band ratio B5/B4. Chlorophyll *a* concentrations used to create the maps were gotten from the linear regression equation for each month;

$$y = \beta x - \alpha$$

Where y is the unknown variable (chlorophyll *a*), β is the slope, x is the pixel value of pixels in the B5/B4 sentinel-2 image and α is the intercept.

The spatial pattern shown by all sampling events showed a high concentration upstream and decreases as you move downstream. This is consistent with the pattern observed with the lab measurements of chlorophyll *a* for Evergreen Lake. The higher concentration of chlorophyll *a* observed upstream might be because the movement of the water is slower upstream due to the lake meandering more upstream and even forming a loop (e.g. where EV8 and EV 9 are located). Another reason might be because the lake is narrower upstream than it is downstream. There is also the presence of more vegetation upstream than there is downstream, and this could contribute to the increase of chlorophyll *a* content upstream.

The September map showed the lowest concentration of chlorophyll *a* distributed across the lakes while August showed the highest concentrations of chlorophyll *a* distributed across the lakes. October 2019 map showed higher concentrations of chlorophyll *a* than October 2018. This

is also consistent with the results observed with the field data. Results of statistical analysis carried out on each map to test the accuracy of the models by comparing the Sentinel-2 estimated chlorophyll *a* and the measured chlorophyll *a* in the laboratory is shown in Table 18. Error analysis including the mean error, mean square error (MSE), root mean squared error (RMSE) and correlation coefficient (r) were conducted. The October and September 2018 models performed better than the other two models, but the September 2018 model had lower MSE and RMSE than the October 2018 model. However, the October 2018 model had a higher R^2 and correlation coefficient than the September 2018 model. The October 2018 model showed a good performance a correlation coefficient of 0.92, bias of 0.31, mean error of 0.10 and RMSE of 4.91. The August 2018 and October 2018 models had MSE and RMSE that are very much higher than the September and October 2018 results.

Table 20

Error Analysis Based on the Comparison Between Interpolated Model Estimation and Field Observed Data

Sampling Event	**Observed Average Chl-a (µg/L)**	**Mean Error (µg/L)**	**Bias (µg/L)**	**MSE $(\mu g/L)^2$**	**RMSE (µg/L)**	**R^2**	**Correlation Coefficient (r)**
August 2018	39.95	0.41	1.02	244.95	15.65	0.34	0.58
September 2018	27.05	-0.11	-0.39	20.89	4.57	0.67	0.81
October 2018	32.85	0.10	0.31	24.08	4.91	0.85	0.92
October 2019	37.35	-0.20	-0.55	198.58	14.09	0.57	0.75

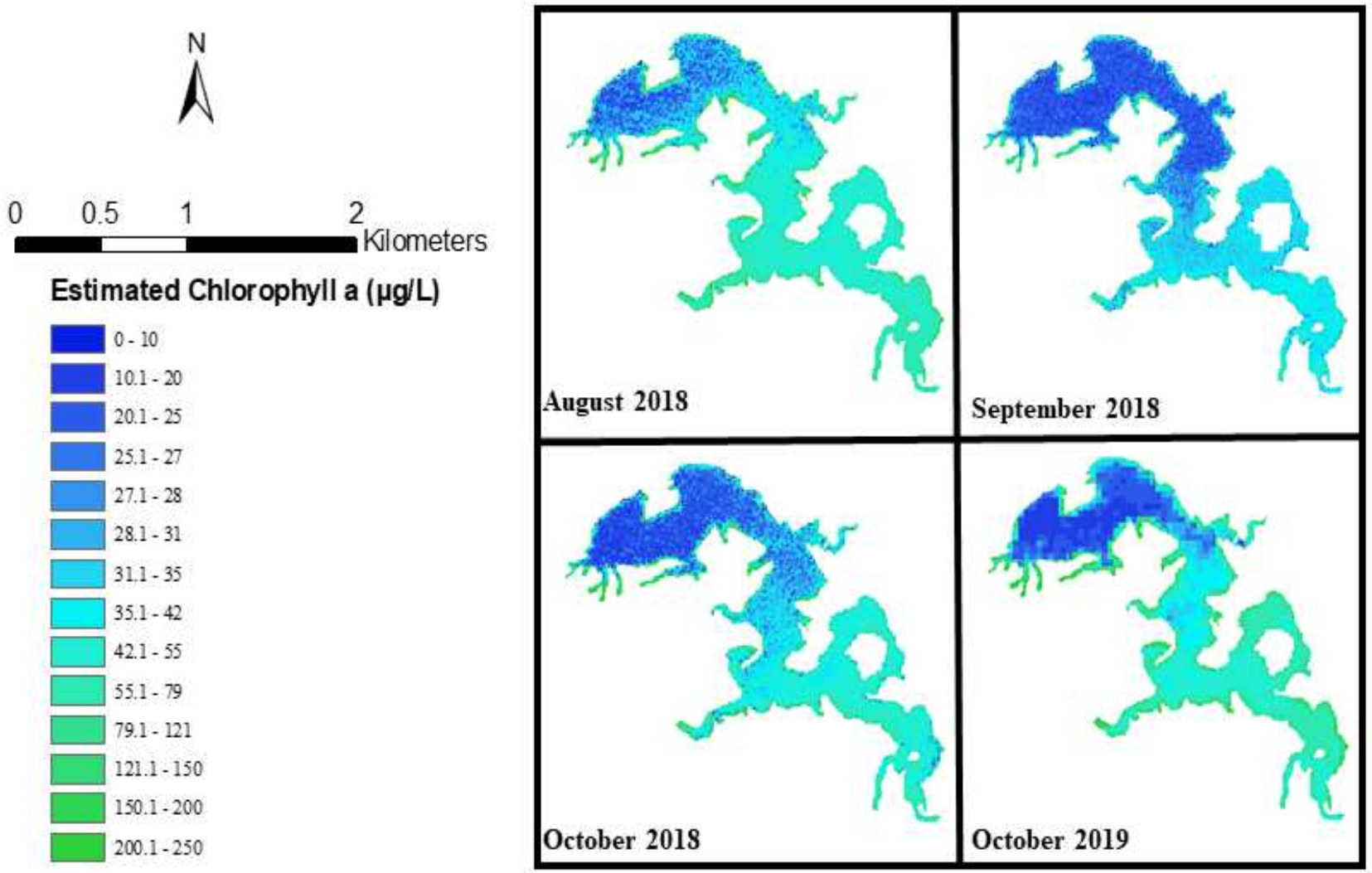

Figure 12. Estimated chlorophyll *a* based on individual sampling events for Evergreen Lake.

CHAPTER VI: CONCLUSION

The temporal distribution of chlorophyll *a* was closely related to that observed for temperature in Lake Bloomington. Chlorophyll *a* was highest in the summer months when temperature was highest and lowest in the fall months when the temperature was lower in Lake Bloomington. For Evergreen Lake, phosphorus was the dominant factor that was closely related to chlorophyll *a*. A higher concentration of phosphorus was observed upstream than downstream, and this same pattern was consistent with the distribution of chlorophyll *a* in Evergreen Lake.

Lake Bloomington showed no strong correlation with the remote sensing data and this could be because of the noise effects induced by the turbidity of the lake. It is difficult to measure the chlorophyll *a* content of small lakes that display high turbidity and since the lake is a small lake, it can easily become turbid with a large influx of sediments into the lake. However, the deep-water zones of Lake Bloomington showed strong correlation relationships when analyzed separately. Evergreen Lake showed a good correlation with the remote sensing data and the results of the analysis showed that there was a general improvement in the relationship between chlorophyll *a* and the satellite reflectance values after atmospheric correction was conducted. Band 5 for the BOA algorithm, B5/B4 for the two-band ratio algorithm and the MCI can be used to carry out chlorophyll *a* analysis for Evergreen Lake. However, the time window between field sampling and satellite overpass time should be limited to ±2 days as better results were observed for time windows that were ±2 days.

Prediction of the chlorophyll *a* concentration of the other locations not sampled was carried out, using ArcGIS tools, after the regression analysis was conducted for Evergreen Lake. Chlorophyll *a* showed a heterogenous spatial pattern where it was higher upstream and lower downstream for Evergreen lake.

REFERENCES

Aggarwal, S., 2004, Principles of remote sensing: Satellite remote sensing and GIS applications in agricultural meteorology, p. 23-38.

Anderson, D. M., Glibert, P. M., and Burkholder, J. M., 2002, Harmful algal blooms and eutrophication: nutrient sources, composition, and consequences: Estuaries, v. 25, no. 4, p. 704-726.

Bartram, J., and Chorus, I., 1999, Toxic cyanobacteria in water: a guide to their public health consequences, monitoring and management, CRC Press.

Braig IV, E. C., Conroy, J., Lichtkoppler, F., Lynch Jr, W. E., and Merchant-Masonbrink, L., 2011, Harmful algal blooms in Ohio waters: Ohio Sea Grant, Fact Sheet OHSU-FS-091-2011, The Ohio State University, Columbus.

Bresciani, M., Cazzaniga, I., Austoni, M., Sforzi, T., Buzzi, F., Morabito, G., and Giardino, C., 2018, Mapping phytoplankton blooms in deep subalpine lakes from Sentinel-2A and Landsat-8: Hydrobiologia, v. 824, no. 1, p. 197-214.

Brezonik, P., Menken, K. D., and Bauer, M., 2005, Landsat-based remote sensing of lake water quality characteristics, including chlorophyll and colored dissolved organic matter (CDOM): Lake and Reservoir Management, v. 21, no. 4, p. 373-382.

Campbell, J. B., and Wynne, R. H., 2011, Introduction to remote sensing, Guilford Press.

Carmichael, W., 2008, A world overview—One-hundred-twenty-seven years of research on toxic cyanobacteria—Where do we go from here?, Cyanobacterial harmful algal blooms: State of the science and research needs, Springer, p. 105-125.

Chen, J., Zhu, W., Tian, Y. Q., Yu, Q., Zheng, Y., and Huang, L., 2017, Remote estimation of colored dissolved organic matter and chlorophyll-a in Lake Huron using Sentinel-2 measurements: Journal of Applied Remote Sensing, v. 11, no. 3, p. 036007.

Clark, J. M., Schaeffer, B. A., Darling, J. A., Urquhart, E. A., Johnston, J. M., Ignatius, A. R., Myer, M. H., Loftin, K. A., Werdell, P. J., and Stumpf, R. P., 2017, Satellite monitoring of cyanobacterial harmful algal bloom frequency in recreational waters and drinking water sources: Ecological indicators, v. 80, p. 84-95.

Collman, R., Cochran, C., and Werner, S., 2002, Soil Survey of McLean County: IL. Technical Report. United States Department of Agriculture: Natural ….

Delegido, J., Verrelst, J., Alonso, L., and Moreno, J., 2011, Evaluation of sentinel-2 red-edge bands for empirical estimation of green LAI and chlorophyll content: Sensors, v. 11, no. 7, p. 7063-7081.

Djamai, N., and Fernandes, R., 2018, Comparison of SNAP-derived Sentinel-2A L2A product to ESA product over Europe: Remote Sensing, v. 10, no. 6, p. 926.

Fu, F. X., Tatters, A. O., and Hutchins, D. A., 2012, Global change and the future of harmful algal blooms in the ocean: Marine Ecology Progress Series, v. 470, p. 207-233.

Glibert, P. M., Anderson, D. M., Gentien, P., Granéli, E., and Sellner, K. G., 2005, The global, complex phenomena of harmful algal blooms.

Gower, J., Doerffer, R., and Borstad, G., 1999, Interpretation of the 685nm peak in water-leaving radiance spectra in terms of fluorescence, absorption and scattering, and its observation by MERIS: International Journal of Remote Sensing, v. 20, no. 9, p. 1771-1786.

Guo, F., Kainz, M. J., Sheldon, F., and Bunn, S. E., 2016, The importance of high□quality algal food sources in stream food webs–current status and future perspectives: Freshwater Biology, v. 61, no. 6, p. 815-831.

Gupta, R. P., 2017, Remote sensing geology, Springer.

Ha, N. T. T., Thao, N. T. P., Koike, K., and Nhuan, M. T., 2017, Selecting the Best Band Ratio to Estimate Chlorophyll-a Concentration in a Tropical Freshwater Lake Using Sentinel 2A Images from a Case Study of Lake Ba Be (Northern Vietnam): ISPRS International Journal of Geo-Information, v. 6, no. 9, p. 290.

Hanna, L. A., 2013, Dissolved and Suspended Sediment Transport Dynamics in Two Agriculturally Dominated Watersheds, McLean County, Illinois, Illinois State University.

Havens, K. E., 2008, Cyanobacteria blooms: effects on aquatic ecosystems, Cyanobacterial harmful algal blooms: state of the science and research needs, Springer, p. 733-747.

Hilborn, E. D., Roberts, V. A., Backer, L., DeConno, E., Egan, J. S., Hyde, J. B., Nicholas, D. C., Wiegert, E. J., Billing, L. M., and DiOrio, M., 2014, Algal bloom–associated disease outbreaks among users of freshwater lakes—United States, 2009–2010: MMWR. Morbidity and mortality weekly report, v. 63, no. 1, p. 11.

Hudnell, H. K., 2008, Cyanobacterial harmful algal blooms: state of the science and research needs, Springer Science & Business Media.

Isenstein, E. M., Trescott, A., and Park, M.-H., 2014, Multispectral remote sensing of harmful algal blooms in Lake Champlain, USA: Water Environment Research, v. 86, no. 12, p. 2271-2278.

Kelly, T., Herida, J., and Mothes, J., 1998, Sampling of the Mackinaw River in central Illinois for physicochemical and bacterial indicators of pollution: Trans Ill State Acad Sci, v. 91, p. 145-154.

Kloiber, S. M., Brezonik, P. L., Olmanson, L. G., and Bauer, M. E., 2002, A procedure for regional lake water clarity assessment using Landsat multispectral data: Remote sensing of Environment, v. 82, no. 1, p. 38-47.

Li, R., and Li, J., 2004, Satellite remote sensing technology for lake water clarity monitoring: an overview: Environmental Informatics Archives, v. 2, p. 893-901.

Lim, J., and Choi, M., 2015, Assessment of water quality based on Landsat 8 operational land imager associated with human activities in Korea: Environmental monitoring and assessment, v. 187, no. 6, p. 384.

Liu, H., Li, Q., Shi, T., Hu, S., Wu, G., and Zhou, Q., 2017, Application of sentinel 2 MSI images to retrieve suspended particulate matter concentrations in Poyang Lake: Remote Sensing, v. 9, no. 7, p. 761.

Main-Knorn, M., Pflug, B., Debaecker, V., and Louis, J., 2015, Calibration and validation plan for the l2a processor and products of the Sentinel-2 mission: International Archives of the Photogrammetry, Remote Sensing & Spatial Information Sciences.

Martimort, P., Arino, O., Berger, M., Biasutti, R., Carnicero, B., Del Bello, U., Fernandez, V., Gascon, F., Greco, B., and Silvestrin, P., Sentinel-2 optical high resolution mission for GMES operational services, *in* Proceedings 2007 IEEE International Geoscience and Remote Sensing Symposium2007, IEEE, p. 2677-2680.

Matthews, M. W., Bernard, S., and Winter, K., 2010, Remote sensing of cyanobacteria-dominant algal blooms and water quality parameters in Zeekoevlei, a small hypertrophic lake, using MERIS: Remote Sensing of Environment, v. 114, no. 9, p. 2070-2087.

Meyers, M. D., 2014, The relationship between environmental factors and cyanobacteria population in Lake Bloomington and Evergreen Lake in McLean County, Illinois.

Muller-Wilm, U., Louis, J., Richter, R., Gascon, F., and Niezette, M., Sentinel-2 level 2A prototype processor: Architecture, algorithms and first results, *in* Proceedings Proceedings of the ESA Living Planet Symposium, Edinburgh, UK2013, p. 9-13.

Olmanson, L. G., Bauer, M. E., and Brezonik, P. L., Use of Landsat imagery to develop a water quality atlas of Minnesota's 10,000 lakes, *in* Proceedings Proceedings of FIEOS 2002, Conference/Land Satellite Information IV/ISPRS Commission I2002, Citeseer.

Park, Y.-J., and Ruddick, K., Detecting algae blooms in european waters, *in* Proceedings ENVISAT Symposium; European Space Agency Special Publication SP-636: Paris, France2007, p. 23-27.

Pettersson, K., 1998, Mechanisms for internal loading of phosphorus in lakes: Hydrobiologia, v. 373, p. 21-25.

Raman, R. K., and Twait, R. M., 1994, Water quality characteristics of Lake Bloomington and Lake Evergreen: ISWS Contract Report CR-569.

Richards, J. A., and Richards, J., 1999, Remote sensing digital image analysis, Springer.

Richardson, L. L., 1996, Remote sensing of algal bloom dynamics: BioScience, v. 46, no. 7, p. 492-501.

Ritchie, J. C., Zimba, P. V., and Everitt, J. H., 2003, Remote sensing techniques to assess water quality: Photogrammetric Engineering & Remote Sensing, v. 69, no. 6, p. 695-704.

Roberts, W. J., 1948, Hydrology of five Illinois water supply reservoirs: Bulletin (Illinois State Water Survey) no. 38.

Stadelmann, T. H., Brezonik, P. L., and Kloiber, S., 2001, Seasonal patterns of chlorophyll a and Secchi disk transparency in lakes of East-Central Minnesota: Implications for design of ground-and satellite-based monitoring programs: Lake and Reservoir Management, v. 17, no. 4, p. 299-314.

Stall, J. B., Rupani, N. L., and Kandaswamy, P., 1958, Sediment transport in money creek: Circular no. 072.

Stevenson, J., 2014, Ecological assessments with algae: a review and synthesis: Journal of Phycology, v. 50, no. 3, p. 437-461.

Stumpf, R. P., Davis, T. W., Wynne, T. T., Graham, J. L., Loftin, K. A., Johengen, T. H., Gossiaux, D., Palladino, D., and Burtner, A., 2016, Challenges for mapping cyanotoxin patterns from remote sensing of cyanobacteria: Harmful Algae, v. 54, p. 160-173.

Toming, K., Kutser, T., Laas, A., Sepp, M., Paavel, B., and Nõges, T., 2016, First experiences in mapping lake water quality parameters with Sentinel-2 MSI imagery: Remote Sensing, v. 8, no. 8, p. 640.

Vesper, D. J., Loop, C. M., and White, W. B., 2001, Contaminant transport in karst aquifers: Theoretical and Applied Karstology, v. 13, no. 14, p. 101-111.

Watanabe, F., Alcantara, E., Rodrigues, T., Rotta, L., Bernardo, N., and Imai, N., 2018, Remote sensing of the chlorophyll-a based on OLI/Landsat-8 and MSI/Sentinel-2A (Barra Bonita reservoir, Brazil): Anais da Academia Brasileira de Ciências, v. 90, no. 2, p. 1987-2000.

Wetzel, R. G., and Likens, G. E., 2013, Limnological analyses, Springer Science & Business Media.

Zhu, W., Yu, Q., Tian, Y. Q., Becker, B. L., and Carrick, H., 2014, Issues and potential improvement of multiband models for remotely estimating chlorophyll-a in complex inland waters: IEEE Journal of Selected Topics in Applied Earth Observations and Remote Sensing, v. 8, no. 2, p. 562-575.